



28 regulation function of wetlands and reservoirs and attest that the combining of wetlands with reservoir  
29 operation cannot fully eliminate the increasing future flood and drought risks. To improve a river basin's  
30 resilience to the risks of future climate change, we argue that implementation of wetland restoration and  
31 development of accurate forecasting systems for effective reservoir operation are of great importance.  
32 Furthermore, this study demonstrated a wetland-reservoir integrated modeling and assessment  
33 framework that is conducive to risk assessment of floods and hydrological droughts, which can be used  
34 for other river basins in the world.

35 **Keywords:** Climate change; Hydrologic projection; Floods and droughts; Wetland hydrological  
36 services; Reservoir operations; Model integration

37

## 38 **1. Introduction**

39 Floods and droughts have produced some of the most frequent and serious disasters in the world  
40 (Diffenbaugh et al., 2015; Hirabayashi et al., 2013; UNISDR, 2015). Globally, they account for 38% of  
41 the total number of natural disasters, 45% of the total casualties, more than 84% of the total number of  
42 people affected, and 30% of the total economic damage caused by all-natural disasters (Güneralp et al.,  
43 2015) in the past. As climate change has been accelerating the hydrological cycle, causing more frequent  
44 and stronger weather extremes, more floods and droughts have been projected to increase at both global  
45 (Chiang et al., 2021; Jongman, 2018) and regional scales (Hallegatte et al., 2013; Wang et al., 2021).  
46 Concurrently, the disaster-related loss of ecosystems (e.g., wetlands, forest, and grassland) and their  
47 services can mitigate the flood and drought risks to a great extent (Gulbin et al., 2019; Walz et al., 2021).  
48 Given this, grey infrastructure such as dams, dikes, and reservoirs, which have often been used to  
49 attenuate flood and drought hazards because of their rapid and visible effects, can play an important role  
50 in ensuring the water security of a river basin (Alves et al., 2019; Casal-Campos et al., 2015). However,  
51 relying solely on grey infrastructure to attenuate floods and droughts has some inadequacies, such as  
52 large investments to build and maintain in addition to adverse effects on downstream ecosystems (Maes  
53 et al., 2015; Schneider et al., 2017). In this context, Nature-based solutions (NBS) for hydro-

54 meteorological hazards mitigation are becoming increasingly popular (Kumar et al., 2021), because  
55 NBS can effectively reduce or even offset the hydrological processes driving floods and droughts (Nika  
56 et al., 2020), while making least disturbance to the environment as well as delivering co-benefits which  
57 grey infrastructure cannot provide (Anderson and Renaud, 2021; Nelson et al., 2020). Therefore, it is  
58 urgent to integrate NBS into the current water management practices to increase basin resilience to  
59 hydrological extremes under climate change.

60 Wetlands have the potential to be used as a NBS for improving water storage and hence the resilience  
61 of a river basin to hydrological extremes along with grey infrastructures (Thorslund et al., 2017). This  
62 is because, similar to man-made dams and reservoirs, wetlands can attenuate flow and alter basin  
63 hydrological processes (Lee et al., 2018), such as floods (Wu et al., 2020a) and baseflows (Evenson et  
64 al., 2015; Wu et al., 2020b). However, unlike man-made grey infrastructures, wetlands are integral in  
65 landscapes and they are connected laterally and vertically with the surrounding terrestrial and aquatic  
66 environments through the hydrological cycling of water and waterborne substances (Åhlén et al., 2020),  
67 making their water storage and cycling fundamental to estimate a watershed's water balance (Golden et  
68 al., 2021; Shook et al., 2021). To understand how and to what extent wetlands can mitigate hydrological  
69 processes, two approaches are commonly used: (i) description of individual wetland **services** at the field  
70 scale (e.g., Park et al., 2014) or wetland scale (e.g., Åhlén et al., 2022); (ii) assessment of wetland  
71 hydrological services at the regional/watershed scale (Fossey et al., 2016; Wu et al., 2020a, 2020b).  
72 **However, the former approach can only be achieved with field observation with instruments and is**  
73 **mainly used to provide key parameters of wetland processes for model calibration (Fossey and Rousseau,**  
74 **2016).** Recently, several wetland modules have been development and coupled to hydrological (e.g.,  
75 Soil and Water Assessment Model, HYDROTEL model) to quantify hydrological function of wetlands,  
76 particularly the mitigation services on floods and droughts (Evenson et al., 2018; Evenson et al., 2016;  
77 Fossey et al., 2015a; Zeng et al., 2020). These wetland hydrological models not only consider the general  
78 water budget of a river basin but also consider the perennial and intermittent hydrological interactions  
79 between wetlands-to-wetlands and wetlands-to- surrounding landscapes. It is of both scientific and  
80 practical interest to project wetland capability in mitigating floods and droughts in response to a

81 changing climate.

82 Reservoirs redistribute large amounts of surface water, thus altering natural hydrological processes,  
83 such as flow range, flood and drought patterns, and basin water balances (Boulangue et al., 2021; Chen  
84 et al., 2021; Manfreda et al., 2021; Zhao et al., 2016). So far, throughout the world, there are 57, 985  
85 reservoirs registered by the International Commission on Large Dams and their total volume has been  
86 reached 14, 602 km<sup>3</sup> (Eriyagama et al., 2020). Such numerous reservoirs and their large storage capacity  
87 should not be neglected in water hazard assessment and hydrological projection because of their  
88 significant modification on flood and drought patterns (Boulangue et al., 2021; Brunner et al., 2021). For  
89 that reason, scholars called for the need to integrate reservoirs in model-based impact analysis of flood  
90 exposure under climate change (Dang et al., 2020a; Yassin et al., 2019). Therefore, there is a growing  
91 need in incorporating reservoir operations into basin hydrologic simulations and predictions.

92 Despite the well-established knowledge of flow regulation and water storage functions that wetlands  
93 and reservoirs can provide in a river basin, most modeling assessments on floods and droughts at the  
94 basin scale do not take the two components into account, or give little emphasis on the combined benefits  
95 of them (Brunner et al., 2021; Golden et al., 2021). Nor are the hydrological processes associated with  
96 these features implicitly included in the calibration of hydrologic models. Recent studies have suggested  
97 that disregarding of the wetlands or reservoir operation would add significant error and larger  
98 uncertainties to simulate hydrologic processes (Brunner et al., 2021; Ward et al., 2020). Because  
99 wetlands are often abundant across many landscapes, which make their water storage and cycling  
100 fundamental to estimate a watershed's water balance (Rains et al., 2016; Lee et al., 2018). Therefore,  
101 missing this component of water balances could potentially lead to disproportionately large model errors  
102 (Rajib et al., 2020). Consequently, integrating the wetlands (Fossey et al., 2015a; Golden et al., 2021;  
103 Rajib et al., 2020) or reservoir operation (Dang et al., 2020; Yassin et al., 2019; Zhao et al., 2016) alone  
104 into watershed-scale hydrologic models may largely minimize uncertainties and improve model  
105 performance. Furthermore, on a global scale, most river basins have wetlands and their river flow has  
106 or will experience reservoir regulation (Muller, 2019; Schneider et al., 2017), which elicits thought-  
107 provoking concerns: What will be the changes of future floods and droughts under the combined

108 influence of wetlands and reservoirs? Such concern is important because the omission of wetlands and  
109 reservoirs can cause the policy-making process to be imprecise at best and ineffective at worst. However,  
110 a reservoir operation and wetland services, integrated basin-scale model rarely exist in the literature.  
111 Furthermore, although few studies (e.g., Rajib et al. (2020; Chen et al., 2021; Wu et al., 2021) provide  
112 insights into modeling and understanding the flow regulation functions provided by wetlands and  
113 reservoirs, however, is it still unclear whether the combining of wetlands with reservoir operation can  
114 largely reduce the risk of future floods and droughts.

115 Considering the above-introduced scientific challenges and management deficiencies, we first  
116 developed a framework of hydrological modeling coupled with wetland modules and reservoir operation  
117 scenarios. We then applied it to a large river basin with abundant wetlands and a large reservoir, the  
118 Nenjiang River Basin in northeast China, to address a central question: Can the combining of wetlands  
119 with reservoir operation largely reduce the risk of future flood and droughts? The Nejinang River Basin  
120 was selected as a case study here because it has abundant wetlands and a large reservoir, and has  
121 undergone intensive anthropogenic activities in the past half century, particularly in the increasing  
122 agricultural water consumption and conversion of wetlands to agricultural and other land uses. Our  
123 framework and results are expected to bring new insights into future floods and droughts and provide a  
124 basis for decision-making to curb the growing impacts of unprecedented and future hydrological  
125 extreme conditions.

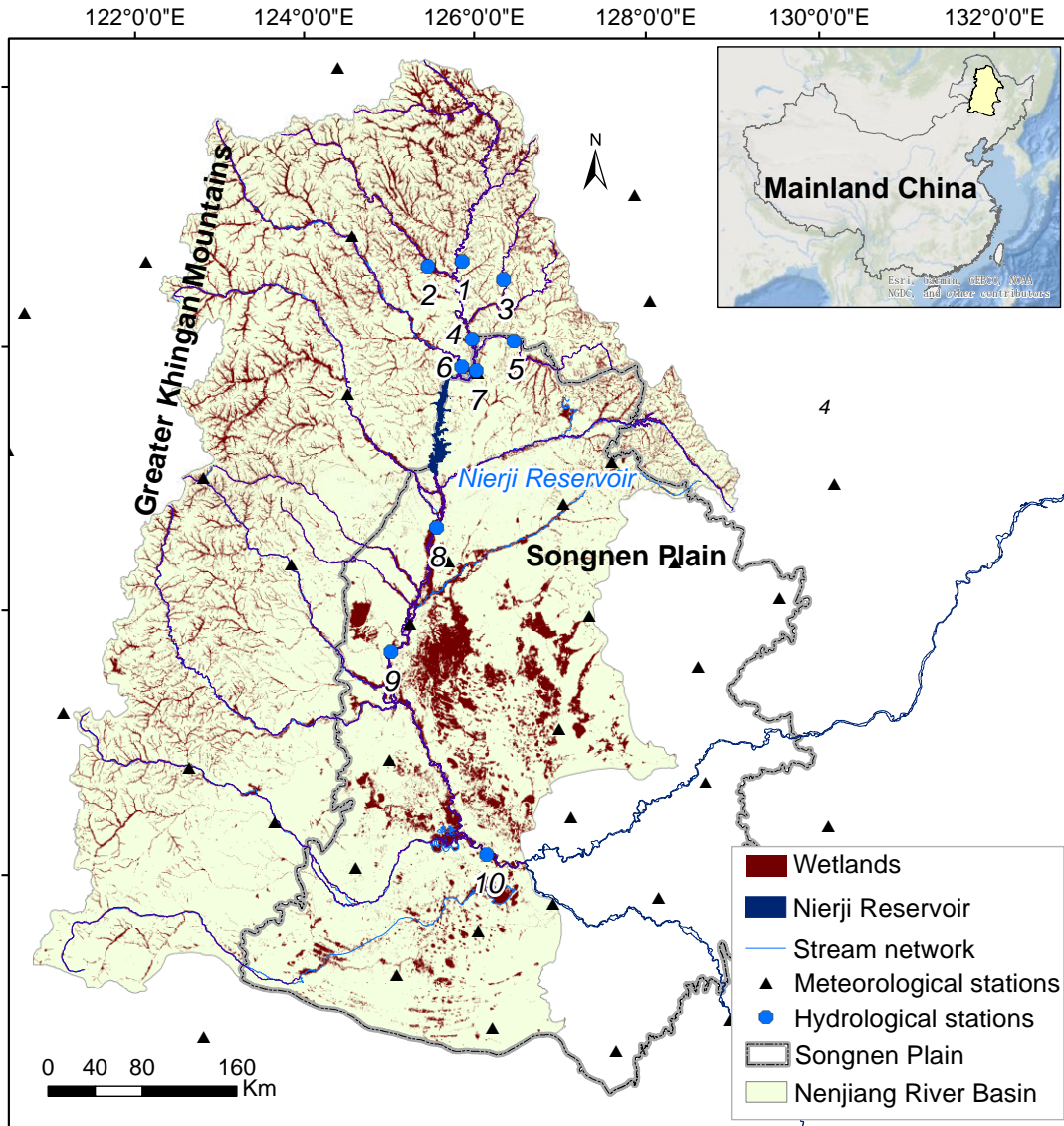
## 126 **2. Methodology**

### 127 2.1 Study area and datasets

128 We conducted this analysis in the Nenjiang River Basin (NRB), a large river basin (291,700 km<sup>2</sup>)  
129 located in the Northeast China (Fig. 1). Long-term annual average runoff depth and volume from the  
130 NRB are 97.4 mm and 22.7 billion m<sup>3</sup>. The river basin is located in the middle-high latitudes and can  
131 be characterized by a temperate semi-humid continental monsoon climate. Inter-annual differences in  
132 temperature and precipitation are large, i.e., disparate hot and cold periods, and uneven dry and wet  
133 conditions (Meng et al., 2019). The average annual temperature across the basin ranges between 2.1-

134 4.5°C. The annual total precipitation within the basin fluctuates from 323.1 to 537.6 mm. Precipitation  
135 is mainly concentrated during June-September, which accounts for about 85% of the annual  
136 precipitation (Li et al., 2014).

137 The NRB is one of the pivotal wetland areas in China. The basin contains several important wetland  
138 conservation areas, among which Zhalong and Nanweng River Wetlands have been designated as a  
139 Ramsar Site of International Importance. The wetlands and their contributing drainage areas (see  
140 Section 2.2.1 for specific definition) within the subbasins monitored by the ten hydrological stations  
141 range from 14 to 23% and from 39 to 56% respectively, demonstrating the large wetland coverage of  
142 the NRB and its sub-basins (Table 1). The lower NRB is an important agricultural area of the Songnen  
143 Plain, which is one of the three major plains (including the Sanjiang, Songnen and Liaohe Plains) in  
144 northeast China. Therefore, understanding potential floods and hydrological droughts under future  
145 climate change is crucial for ensuring regional food security and wetland ecological integrity. During  
146 the past 60 years, land use and land cover types have drastically changed owing to large-scale  
147 development of intensive agriculture and water resources management (Meng et al., 2019). The area of  
148 wetlands in the NRB decreased by nearly 23% from 1978 to 2000 (Chen et al., 2021), with only 16.34%  
149 remaining today (Table 1), which largely degraded their services (Wu et al., 2021). Along with the  
150 reduction in wetland area, the hydrological functions of wetlands in the NRB, such as water storage,  
151 flood mitigation and baseflow support, have been considerably reduced (Wu et al., 2021). These wetland  
152 services are closely related to flood and drought risks, such as the 1998 mega-flood. In order to  
153 effectively deal with the risk of floods and droughts, the Nierji Reservoir was constructed along the  
154 mainstream NRB (Fig. 1); it started normal operation in 2006. The drainage area of the reservoir  
155 accounts for 22.8% of the NRB. The Nierji Reservoir, located in the upper Nenjiang River (Fig. 1), has  
156 flood control and water supply as the primary purposes and hydropower generation and navigation as  
157 secondary purposes, thus playing an important role in the distribution of water resources for the lower  
158 NRB.



159  
 160 **Figure 1. Location of the Nenjiang River Basin and the distribution of wetlands, river networks, Nierji**  
 161 **Reservoir, and hydrological and meteorological stations within the basin.**

162

163 Table 1 The drainage area of the ten hydrological stations used in this study, area ratios of wetlands and  
 164 their contributing areas to the drainage area of the Nenjiang River Basin, northeast China.

ID	River	Hydrological stations	Drainage area (km <sup>2</sup> )	Wetland area ratio (%)	Wetland contribution area ratio (%)
1	Mainstream	Shihuiyao	17205	22.2	54.7

2	Duobukuli River	Guli	5490	16.3	57.1
3	Menlu River	Huolongmen	2151	20.8	50.7
4	Mainstream	Kumotun	32229	20.4	54.3
5	Keluo River	Kehou	7310	23.4	56.2
6	Gan River	Liujiatun	19665	13.2	49.9
7	Mainstream	Nenjiang	61249	18.3	54.1
8	Mainstream	Tongmeng	108029	13.1	47.5
9	Mainstream	Fulaerji	123911	13.7	39.0
10	Mainstream	Dalai	221715	16.3	42.4

165

166 The driving datasets used in this study include meteorological data, land-use/land-cover types, soil  
167 texture, digital elevation models, drainage network, and observed discharge data. The land-use/land-  
168 cover types for 2015 (including wetland types), digital elevation models and digital elevation models  
169 with 1 km resolution were obtained from Resource and Environment Science and Data Center  
170 (<https://www.resdc.cn/>). The river network was collected from the Geographical Information  
171 Monitoring Cloud Platform (<https://www.dsac.cn/DataProduct/Index/30>). Historical daily  
172 meteorological datasets including precipitation and air temperature for the period 1963-2020 were  
173 obtained from 39 weather stations administered by the National Meteorological Information Centre of  
174 China (<http://data.cma.cn>) and 49 weather stations in the upper NRB (Fig. 1) administered by the  
175 Nenjiang Nierji Hydraulic and Hydropower Ltd. Company (<http://www.cnnej.cn>). The hydrological  
176 data from ten hydrological stations (see Fig.1 and Table 1) were obtained from the Songliao Water  
177 Resources Commission, Ministry of Water Resources (<http://www.slwr.gov.cn/>), with the time series  
178 extending from 1963 to 2020.

179 In this study, we drove hydrological model using five GCM projections (GFDL-ESM4, IPSL-CM6A-  
180 LR, MPI-ESM1-2-HR, MRI-ESM2-0, UKESM1-0-LL) under three Socioeconomic Pathways (SSPs)  
181 from the latest CMIP6 (O'Neill et al., 2016). Each of these specific SSPs represents a development  
182 model that includes a corresponding combination of development characteristics and influences. The



183 three SSPs that were used herein include SSP126, SSP370 and SSP585, which represent potential  
184 futures characterized by green-fueled growth (van Vuuren et al., 2017), high inequality between the  
185 countries (O'Neill et al., 2016) and fossil-fueled growth (Kriegler et al., 2017), respectively. We chose  
186 the five GCM projections because their high resolution (0.25°) and wide application in previous studies.  
187 Given the data requirements of the hydrological model, we downloaded the SSP outputs including daily  
188 precipitation, maximum and minimum temperature. We then performed bias correction and spatial  
189 downscaling of the SSP outputs. The bias correction of SSP outputs was carried out using the CMhyd  
190 software (<https://swat.tamu.edu/software/cmhyd>), in which the widely used Delta Change method in the  
191 CMhyd software was adopted. Delta Change bias-corrects the projected SSP outputs based on the  
192 historical statistics and thus conserves the linear spatial-, temporal-, and multi-variable dependence  
193 structure in the future climate (Bosshard et al., 2011; Maraun, 2016; Moore et al., 2008; Shafeeque and  
194 Luo, 2021). The ANUSPLIN package developed by (Hutchinson and Xu, 2004) was then used to  
195 uniformly downscale the output from five bias-corrected GCMs to a resolution of 1-km based on the  
196 DEM. Following previous studies (Hagemann and Jacob, 2007; Zhao et al., 2021), the multi-model  
197 ensemble means ( $M_{GCM}$ ) of the daily precipitation, and the maximum and minimum temperature under  
198 the SSPs scenarios were then obtained to diminish the uncertainties inherited in a single GCM. MEM  
199 was calculated using an equally-weighted average:

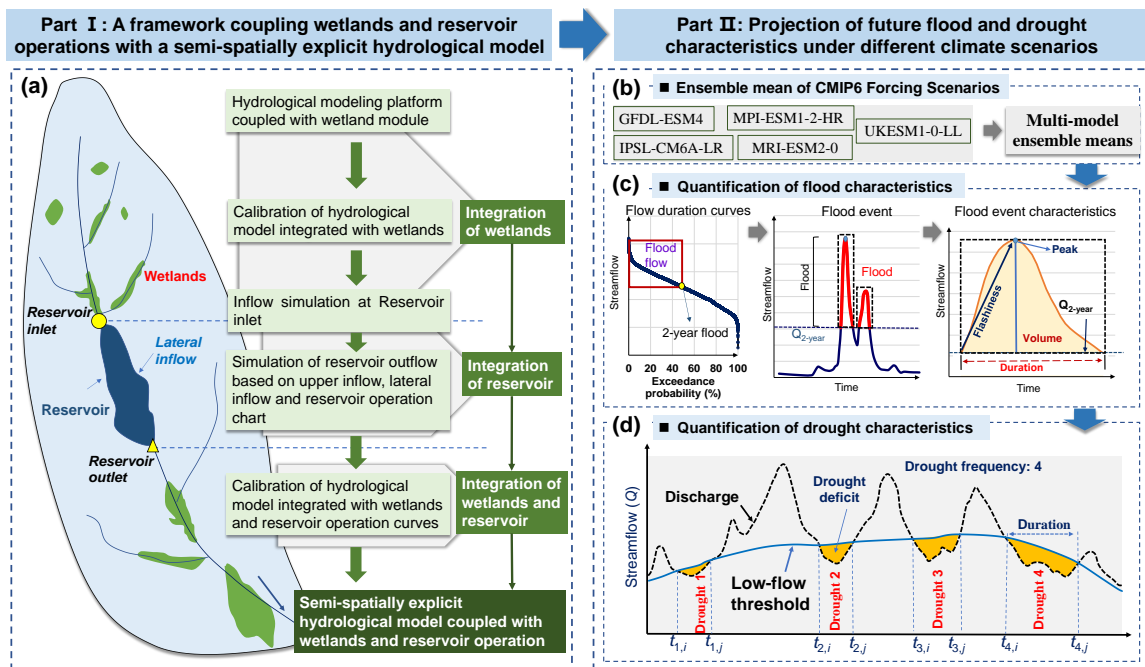
$$200 \quad M_{GCM} = \frac{1}{N} \sum_{i=1}^N P_i \quad (1)$$

201 where  $M_{GCM}$  is the multi-model ensemble means,  $N$  is the number of ensemble members (5 in this study);  
202 and  $P_i$  is the projected climate data of an ensemble member. In this study, the  $M_{GCM}$  of five GCMs were  
203 used to drive hydrological modeling.

## 204 2.2. Framework of hydrological modeling coupled with wetland modules and reservoir operation 205 scenarios

206 We developed a spatially-explicit hydrological modeling framework that considers wetland  
207 hydrological processes and reservoir operations based on HYDROTEL model and reservoir simulation  
208 algorithms (Fig.2). Such a modeling framework was based on a distributed coupling implementation at

209 watershed scale from upstream to downstream. Observed streamflow from seven hydrological stations  
 210 (see hydrological stations 1-7 in Fig.1) located upstream of the Nierji Reservoir and three hydrological  
 211 stations (see hydrological stations 8-10 in Fig.1) installed at downstream of the reservoir, respectively,  
 212 were used to calibrate the HYDROTEL model. For the upstream Nierji Reservoir, we calibrated the  
 213 HYDROTEL model against observed streamflow of seven hydrological stations with consideration of  
 214 wetlands (i.e., hydrologic-wetlands model). Among the seven hydrological stations, the Nenjiang  
 215 Station is located at the end of the upstream, where the simulated streamflow was taken as the inflow of  
 216 the reservoir. We then computed the reservoir outflow using the simulated inflow, estimated lateral  
 217 inflow and reservoir simulation algorithms (see Section 2.2.2), thereby integrating reservoir operation  
 218 into the hydrologic-wetlands model to build a hydrologic-wetlands-reservoir model. Based on the  
 219 calibrated hydrologic-wetlands-reservoir model, we simulated the outflow of the reservoir (Sect. 2.2.2),  
 220 which was used as the input streamflow for downstream model calibration. For the downstream reservoir,  
 221 we calibrated the hydrologic-wetlands-reservoir model against observed streamflow of Tongmeng,  
 222 Fulaerji and Dalai Stations. Based on this framework, the simulation of basin hydrological processes  
 223 coupled with basin scale wetlands and reservoir operations were realized.



224  
 225 Figure 2. Framework for projecting future flood and hydrological droughts based on a semi-spatially

226 integrating wetlands and reservoir operation into a basin hydrological model: (a) a framework coupling  
227 wetlands and reservoir operations with a semi-spatially explicit hydrological model; (b) multi-model  
228 ensemble means from five GCM projections used for driving modeling framework; (c) methodology  
229 for determining a flood threshold, defining flood events, and extracting flood characteristics, and (d) a  
230 sequence of runs with examples of drought deficit, duration, and frequency.

#### 231 2.2.1. A semi-distributed hydrological model platform coupled with wetland modules

232 The PHYSITEL/HYDROTEL modeling platform coupled with two wetland modules (isolated and  
233 riparian wetlands) (Fossey et al., 2015b), has been used to quantify hydrological function of wetlands  
234 (e.g., Fossey and Rousseau, 2016; Blanchette et al., 2019; Wu et al., 2023). PHYSITEL is a Geographic  
235 Information System based pre-processing platform for managing hydrological modeling data (Noël et  
236 al., 2014; Rousseau et al., 2011). Using general basin data (a digital elevation model, vectorized river  
237 network and lacustrine water bodies, and raster-based land use and soil matrix distribution maps),  
238 PHYSITEL divides the basin into more detailed hydrological response units, i.e., relatively  
239 homogeneous hydrological units (RHHUs) (Fortin et al., 2001). The RHHUs were defined using the  
240 algorithm for delineating and extracting hillslopes proposed by (Noël et al., 2014). The hillslopes with  
241 same characteristics (e.g., physical geography and hydrological response) were then aggregated within  
242 each RHHUs. In addition, the PHYSITEL platform distinguishes wetlands from other land-use types,  
243 and then classifies both isolated and riparian wetlands based on an adjacency threshold (i.e., percentage  
244 of pixels in contact) between the wetlands and the river network (Fossey et al., 2015b). Specifically, if  
245 more than adjacency threshold (e.g., 1%) of wetland pixels are connected to the river network, they are  
246 considered as pixels of a riparian wetlands; otherwise, they are referred to as isolated wetlands. It  
247 subsequently generates data pertaining to isolated and riparian wetlands and their contributing areas.  
248 The contributing area of wetlands is defined as the sum of the area of all wetland RHHUs and upland  
249 RHHUs within their immediate catchment areas situated along active fill-spill pathways to the stream  
250 network (Evenson et al., 2016). The PHYSITEL platform uses the concept of a hydrologically  
251 equivalent wetland (HEW) proposed by (Wang et al., 2008) to integrate isolated and riparian wetlands  
252 at the RHHU scale. These typically large RHHUs contain large wetland complexes consisting of various

253 wetland categories such as bogs, fens, marshes, and forested peatlands. After defining the hydrological  
254 and wetland parameters, PHYSITEL can directly export the database as part of the input data to  
255 HYDROTEL; these data can also be used for other watershed hydrological models.

256 HYDROTEL is a physically-based and semi-distributed hydrological model (Bouda et al., 2014;  
257 Bouda et al., 2012; Turcotte et al., 2007) that requires wetland parameter data, land-use type maps, soil  
258 texture maps, meteorological data (e.g., daily temperature and precipitation) and daily flows as input.  
259 The HYDROTEL model couples the hydrological processes associated with both isolated and riparian  
260 wetlands (i.e., the isolated and riparian wetlands modules) at the RHHU scale and calculates the wetland  
261 water balance with respect to the surface area of the HEW, contribution area and RHHU. Specifically,  
262 for isolated wetlands, the hydrogeological processes are integrated in the vertical water budget (Fortin  
263 et al., 2001) at the RHHU scale. For riparian wetlands, the water balance is partially integrated in the  
264 vertical water budget of an RHHU and directly connected to the associated river segment via the  
265 kinematic wave equation (Beven, 1981). Based on this, the isolated wetlands modules can realize the  
266 vertical water balance processes of hillslope wetlands with land surface runoff processes, while the  
267 riparian wetlands modules can realize the interaction of hydrological processes between riparian  
268 wetlands and river channels. It should be mentioned that the HEW concept developed by Wang et al  
269 (2008) served as the foundation for the integration of riparian wetlands and isolated wetlands into the  
270 modeling framework. This concept contends that the features of one HEW (also known as an isolated  
271 wetland or riparian wetland) are equivalent to the sum of the characteristics of each wetland inside a  
272 RHHU (which could either be hill slopes or elementary sub-watersheds related to one river segment).  
273 The following premises apply to this concept: (i) only one isolated and/or riparian HEW per RHHU; (ii)  
274 one HEW can be fully integrated within a RHHU; (iii) isolated HEW parameters must be numerically  
275 integrated; and (iv) riparian HEW parameters must be numerically integrated and spatially integrated  
276 (i.e., located in a specific location on the river segment). Therefore, isolated wetlands and riparian  
277 wetlands do not appear to have direct hydrological connection within a RHHU. However, isolated  
278 wetlands also have hydrological interactions with riparian wetlands through vertical water balance  
279 processes and fill-spill processes (Fossey et al., 2015). Nevertheless, such representations provide a

280 modelling approach that can simulate water balances at the wetland scale while considering their  
281 interactions with the surrounding environment (contributing drainage area and hydrological  
282 connectivity) (Fossey et al., 2015b). But the hydrological interactions between riparian wetlands and  
283 isolated wetlands are not considerate in this study.

#### 284 2.2.2. Simulation of Nierji reservoir operations

285 Based on the simulated runoff at the inlet (the Nenjiang Station), lateral inflow, and the schemes of  
286 reservoir operation, we estimated the reservoir outflow using the ResSimOpt-Matlab software package  
287 developed by Dobson et al., 2019. ResSimOpt-Matlab contains three algorithms for reservoir simulation.  
288 The first algorithm considers a case when we want to always release a constant amount over the  
289 simulation period. This constant amount is the target release that would cover all downstream demand  
290 for water, for instance for domestic use and/or irrigation. The second consider a case when we still want  
291 to release the target demand but we would also like to (1) apply some hedging (that is, an intentional  
292 reduction of the release - even if it would still be feasible to release the target demand - aimed at saving  
293 more water and thus facing smaller deficits at later time); and (2) attenuate downstream peak flows for  
294 flood control purpose. The third algorithm, which was used in this study, dynamizes the operation rules.  
295 A dynamic operation schemes was used in this study to achieve the simulation. Specifically, following  
296 (Dobson et al., 2019) and according to actual hydrological conditions, we defined two seasons: the wet  
297 season (from June to September) when the risk of flooding is higher and we wanted to release the target  
298 demand and provide some storage space for flood control, and the dry season when the risk of flooding  
299 is low and the main objective is to sustain ecological baseflows. The required input data to the algorithm  
300 includes reservoir inflow ( $Q_{in}$ ) ( $m^3/s$ ), the minimum environmental flow ( $E_{env}$ ), ( $m^3/s$ ) initial storage ( $S_0$ )  
301 ( $m^3$ ), minimum ( $S_{min}$ ) and maximum ( $S_{max}$ ) storage ( $m^3$ ), estimated evaporative losses ( $E_{vap}$ ) (mm),  
302 released discharge ( $Q_{out}$ ) ( $m^3/s$ ) and the simulation time-step length (day). Based on the required data,  
303 we performed reservoir simulation by implementing the mass balance equation at each simulation time  
304 step  $t$ :

$$\begin{cases}
S_{(t+1)} = S_{(t)} + Q_{in(t)} - E_{vap(t)} - Q_{out(t)} & \text{or} & S_{(t)} + Q_{in(t)} - E_{min(t)} - E_{vap(t)} \\
0 \leq S_{(t)} \leq S_{max} \\
0 \leq R_{(t)} \leq \min(S_{(t)} + Q_{in(t)} - E_{min(t)} - E_{vap(t)}, Q_{max})
\end{cases} \quad (2)$$

306 where  $S_t$  is the reservoir storage at time  $t$ .  $S_t$  and  $Q_{out}$  are constrained by the design specifications  
307 and operation rules of a reservoir. Specifically,  $S_t$  cannot exceed the reservoir capacity  $S_{max}$ , while  
308  $Q_{out}$  ( $m^3/s$ ) is constrained by the operation schemes and capacity of the turbines  $Q_{max}$  ( $m^3/s$ ). The  
309 excess water, if any, is spilled:

$$Q_{spill(t)} = \max(S_{(t)} + Q_{in(t)} - E_{vap(t)} - Q_{out(t)}) \quad (3)$$

311 Based on this, the dynamic  $Q_{out}$  can be represented using the equation (1) and (2).

312 We collected information on the reservoir operation including reservoir capacity, control water levels,  
313 outflow, the storage-area-water level relationship, the tailwater level-discharge relationship, and the  
314 maximum release, along with other data necessary to estimate the outflow. The reservoir inflow is the  
315 simulated streamflow at the Nengjiang Hydrological Station, which is at the inlet of the Nierji Reservoir.  
316 The minimum storage and maximum storage are 4.9 billion  $m^3$  and 86.1 billion  $m^3$ , respectively. Based  
317 on the available data for the study area, the Karrufa method (Kharrufa, 1985) was used to estimate daily  
318 evaporative losses from the reservoir. We convert days to seconds so that it would correspond to the  
319 flow data. During the wet season, the actual operation schemes for the Nierji Reservoir are as follows:  
320 The pre- and post-flood periods are June 1-20 and September 6-30, respectively, with a flood limited  
321 water level of 216.0 m; The main flood period is from June 21 to August 25, and the reasonable flood  
322 limited water level ranges from 213.4 m to 216.0 m and can be gradually increased. During the dry  
323 season, the environmental flow was defined as 25.3% of the daily streamflow during the dry season  
324 over the years based on the designed operating curves of the reservoir operation chart.

### 325 2.2.3. Model calibration, validation and performance assessment

326 For all above scenarios, we calibrated the HYDROTEL model against observed streamflow at a daily  
327 time step over 8 years, including a 1-year warm-up (2010.10.01-2011.09.30) and a 7-year calibration  
328 (2011.10.01-2018.09.30) periods. The same model settings (i.e., key parameters, simulation periods,

329 fitting algorithm, and objective function, etc.) were used for the calibration processes under the both  
330 presence and absence scenarios. Following (Arsenault et al., 2018), the model was calibrated using full-  
331 time observations without additional validation, as the former allows for more reliable parameters and  
332 maximizes the accuracy of the model. The dynamically dimensioned search algorithm (DDS) developed  
333 by (Tolson and Shoemaker, 2007) was used to calibrate the 13 most sensitive parameters of the model  
334 as proposed by (Foulon et al., 2018). Based on the maximizing of Kling-Gupta efficiency (KGE) (Gupta  
335 et al., 2009), automatic calibrations using DDS were carried out utilizing 10 optimization trials (250 sets  
336 of parameters per trial). Then, the best set of parameter values out the 10 trials were selected following  
337 (Foulon et al., 2018). The KGE was chosen as the objective function because previous research has  
338 shown that it can improve flow variability estimates when compared to the Nash-Sutcliffe efficiency  
339 (NSE) (Fowler et al., 2018; Garcia et al., 2017).

340 It should be noted that we calibrated the HYDROTEL model against observed streamflow under with  
341 and without wetland scenarios. For the without wetland scenarios are defined as follows: When the  
342 wetland modules are turned off in HYDROTEL, wetland areas are not removed, but they are treated as  
343 the land cover of saturated soils. Such a saturated soil is fixed and does not participate in hydrological  
344 processes such as water yielding and runoff routing, and thus their explicit storage properties are not  
345 accounted for in the modeling. This is a basic assumption that has been used in several studies using  
346 models such as SWAT (Liu et al., 2008; Wang et al., 2008; Evenson et al., 2015), Mike 11 (Ahmed,  
347 2014) and HYDROTEL (Fossey et al., 2016; Fossey and Rousseau, 2016a, b; Wu et al., 2019, 2020a,  
348 2021), to quantify the hydrologic services provided by wetlands (flood mitigation, flow regulation and  
349 baseflow support etc.).

350 To determine whether coupling the wetland module and the reservoir can improve the model  
351 performance, we compared (1) the efficiency of the model in simulating daily flow processes; and (2)  
352 the capability of the model to simulate floods and hydrological droughts in the presence or absence of  
353 the wetlands and the combination of wetlands and reservoir. Following the recommendations of (N.  
354 Moriasi et al., 2007) and (Moriasi et al., 2015), four performance criteria were selected to assess model  
355 performance with regards to simulated daily flows with and without the presence of the wetland modules

356 and reservoir operation, namely the NSE (Nash and Sutcliffe, 1970), Correlation Coefficient (CC), the  
357 root-mean square error (RMSE) and the percent bias (Pbias). We used multiple performance criteria  
358 because it may be unreliable to rely on a single objective function to determine whether the model  
359 performs well (Fowler et al., 2018; Pool et al., 2018; Seibert et al., 2018). It should be noted that although  
360 NSE as an objective function has shortcomings in model calibration, it can still provide an important  
361 reference for the evaluation of simulation results as a performance criterion as suggested by Moriasi et  
362 al. (2007, 2015). In addition, we compared model performance considering daily hydrograph changes.  
363 Furthermore, flood and drought features were extracted (see Sect. 2.4.2 and 2.4.3) and used to discern  
364 whether, and to what extent, the coupled wetland modules and reservoir simulations could improve the  
365 model's ability to simulate droughts and floods.

366

### 367 2.3. Projection of future flood and drought characteristics under different climate scenarios

368 The calibrated hydrologic-wetland-reservoir model was used to simulate streamflow driven by multi-  
369 model ensemble means from the latest CMIP6 and to derive drought and flood characteristics. The flood  
370 and drought characteristics were then compared against historical periods (1971-2020) to discern how  
371 future hydrological extremes will be changed under the influence of wetlands and reservoirs (see Part  
372 II in Fig.2).

373 The future simulated streamflow at the Nenjiang and Dalai hydrological stations driven by the  
374 ensemble mean of bias-corrected CMIP6 Forcing Scenarios (see Section 2.1) were selected to derive  
375 drought and flood characteristics. The Nenjiang Station was chosen because it is located at the outlet to  
376 (mouth of) the upper NRB and the inlet to the Nierji Reservoir, whose flood and drought patterns are  
377 mainly driven by wetlands and climate change. Moreover, changes in drought and flood characteristics  
378 of the Nenjiang Station are critical to the operation of the reservoir immediately lower reach. The Dalai  
379 Station, located at the outlet of the entire NRB, was used as a proxy to characterize future flood and  
380 drought evolution for the whole basin under the combined influence of the wetlands and reservoir. Using  
381 the calibrated hydrologic-wetland-reservoir model, we carried out the simulation of hydrological  
382 processes for the historical period and under the constraints of the SSP126, SSP370 and SSP585



383 scenarios. We then extracted flood and hydrological drought characteristic indices from the simulations  
384 to conduct a comparative analysis of their temporal evolution for the near-future (2026-2050), mid-  
385 century (2051-2075) and end-century (2076-2100). The purpose of subdividing the analysis into three  
386 time periods was to compare whether, or to what extent, flood and drought characteristics increase or  
387 decrease for different future time periods as compared to a historical period.

388 In this study, we characterized floods in terms of four indices consisting of flood peak, flood volume,  
389 duration, and flashiness (Fig. 2c). The 2-year flood streamflow was used as a threshold for defining  
390 flood events, as it has been often used as a substitute of the threshold for bankfull discharge in previous  
391 studies (Cheng et al., 2013; Wu et al., 2020; Xu et al., 2019). Daily streamflows that were greater than  
392 the 2-year flood threshold were considered as flood flows. Flood flows occurring on multiple  
393 consecutive days were considered as a single flood event. The flood indices, i.e., flood peak, volume,  
394 duration, and flashiness were derived with respect to event hydrographs. Flood volume is the cumulative  
395 flow from the initial to the end of a flood event with respect to the 2-year flood streamflow level, and  
396 represents the flood intensity for different flood events (Wang et al., 2015). The annual total flood  
397 volume is the total amount of water associated with all flood events during a water year. We calculated  
398 the annual total flood volume based on flood duration and the average amount of streamflow per event  
399 in a water year. Flood duration varies for different floods and is, therefore, an important characteristic  
400 of a flood event. We summed the flood duration of each event in a water year to obtain the annual flood  
401 days. In addition, the annual maximum peak flow was derived from the daily flows to investigate  
402 changes in the characteristics of extreme floods. We extracted the 2-year flood threshold for a  
403 hydrological station based on the streamflow-exceedance probability curve. Flashiness is a measure of  
404 flood severity and is defined as the difference between the peak discharge and action stage discharge  
405 normalized by the flooding rise time (Saharia et al., 2017).

406 We characterized hydrological drought characteristics using four indices consisting of the number of  
407 droughts, annual drought days, drought duration and deficit (Fig. 2d). A threshold method was used to  
408 define hydrological drought events because it can determine the start and end of a hydrological drought  
409 event, which allows further assessment of drought characteristics, such as frequency, duration, and

410 intensity of a drought event (Cammalleri et al., 2017). It is based on defining a flow threshold (discharge,  
 411  $Q$ ,  $m^3/s$ ), below which a hydrological drought event is considered to occur (also known as a low flow  
 412 spell). A daily variable threshold, defined as an exceedance probability of the 365 daily flow duration  
 413 curves was used to derive drought events from daily streamflow records (Fleig et al., 2006; Hisdal and  
 414 Tallaksen, 2003). For rivers with perennial flow, relatively low streamflows ranging from  $Q_{70}$  to  $Q_{95}$   
 415 have been used as a reasonable threshold (Tallaksen and van Lanen, 2004; Zelenhasić and Salvai, 1987).  
 416 In this study, we chose the 90th percentile ( $Q_{90-n}$ ) streamflow as the daily threshold, which also used as  
 417 the threshold for identifying droughts in future climate change scenarios. The  $Q_{90-n}$  of all days was  
 418 determined based on the observed historical daily streamflow.

419 To enable the comparison across different modeling scenarios (i.e., historical scenarios and future  
 420 climate change scenarios), we derived drought days, deficit, duration, and number from identified  
 421 hydrological drought events to characterize their patterns. Drought volume deficit was calculated by  
 422 subtracting daily streamflow from the threshold level ( $Q_{90-n}$ ) during a drought event, and it presents the  
 423 severity of the drought compared to the normal streamflow conditions. Drought duration was the  
 424 cumulative number of days during a drought event, i.e., the number of days from the beginning to the  
 425 end of the drought. Annual drought days were then the cumulative drought duration in a year. The  
 426 number of droughts is expressed by the number of drought events during a study period. In addition, the  
 427 annual minimum flows of each water year were extracted and used to determine the model's ability to  
 428 simulate very low flows. The drought volume deficit was calculated as:

$$429 \quad D_k = \sum_{t_i}^{t_j} (Q_{90,t} - Q_n) \cdot 60 \cdot 60 \cdot 24 \quad (4)$$

430 where  $D_k$  is the drought volume deficit ( $m^3$ ) of a drought event  $k$  at a hydrological station and  $t_{k,i}$  and  $t_{k,j}$   
 431 are the initial and final time steps of the run, respectively.  $Q_n$  is the daily streamflow of  $n$  day of the year  
 432 (1-365). The corresponding drought duration is computed as  $t_j - t_i + 1$ .

433 For hydrological drought events that occur relatively close in time, the inter-event time method  
 434 introduced by (Zelenhasić and Salvai, 1987) was used to separate events. This method defines a  
 435 minimum gap period,  $t_c$ , and assumes that if the inter-event time  $(t_j - t_i + 1) < t_c$ , then the consecutive events

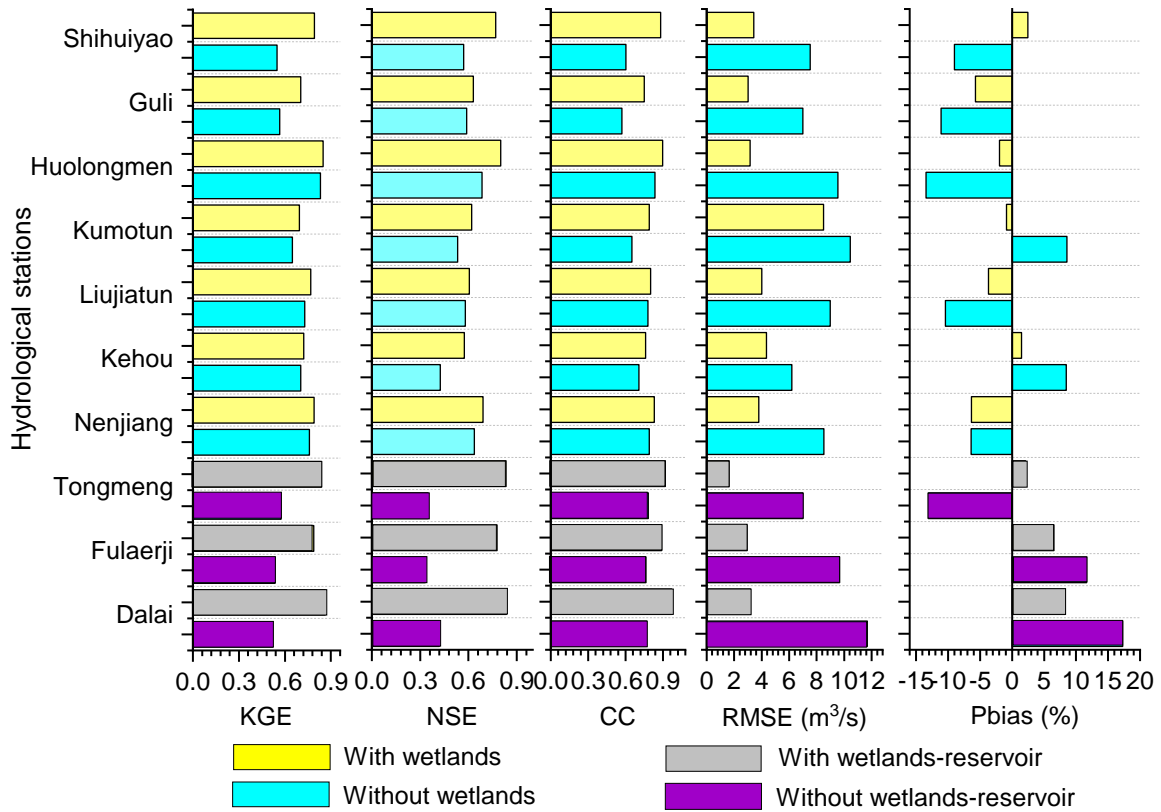
436 are interdependent and merged. In this case, the total drought deficit volume is the sum of the individual  
437 deficit values, and the event duration is the so-called real drought duration (sum of the single event  
438 duration, excluding excess periods). For this study,  $t_c$  was set equal to 7 days as recommended by  
439 (Cammalleri et al., 2017).

440

### 441 **3. Results**

#### 442 3.1 Model performance on daily streamflow and hydrography

443 Fig. 3 depicts model performances for calibration results in the presence or absence of the wetlands  
444 and the combination of wetlands and reservoir at the ten hydrological stations in the NRB. In the case  
445 of whether the wetlands were present or absent, the simulated daily streamflow results all achieved the  
446 acceptable performance criteria ( $NSE > 0.5$  and  $Pbias \leq \pm 15\%$ ) suggested by (Moriiasi, 2007) and  
447 (Moriiasi et al., 2015) at the Shihuiyao, Guli, Huolengmen, Kumotun, Kehou, Liujiatun and Kumotun  
448 stations. However, compared with the calibrated results of the model without wetlands, the simulation  
449 efficiency under with wetland scenario improved to varying degrees. Specifically, the relative  
450 improvement (i.e., the relative change) of KGE values at Shihuiyao, Guli, Huolengmen, Kumotun,  
451 Kehou, Liujiatun, Kumotun, Tongmeng, Fulaerji and Dalai were 44%, 24%, 2%, 6%, 5%, 3%, 4%, 46%,  
452 47% and 67%, respectively. In addition, the NSE and CC values were generally larger in the presence  
453 of wetlands than those in the absence of wetlands, and the RMSE and Pbias values are generally smaller  
454 than those in the absence of wetlands, showing that integrating wetlands into the hydrological model  
455 can slightly improve the model calibration results.



456

457

Figure 3. Model performances for calibration results for the with/without wetlands and reservoir

458

scenarios at the ten hydrological stations in the Nenjiang River Basin. The KGE, NSE, CC, KGE,

459

RMSE and Pbias refer to Kling-Gupta efficiency, Nash-Sutcliffe efficiency, Correlation Coefficient,

460

Root Mean Square Error, and the percentage bias, respectively.

461

462

For the lower reaches of Nierji Reservoir (i.e., the Tongmeng, Fulaerji and Dalai stations, representing

463

inclusion of the wetlands and the reservoir operation into hydrological modeling), the NSE and CC

464

values were greatly higher and RMSE and Pbias values were substantially lower when the wetlands and

465

reservoir were considered, in comparison to the case without wetlands-reservoir (Fig. 3). In fact, in the

466

scenario without wetlands-reservoir, the simulated daily streamflow results failed the acceptable

467

performance criteria ( $NSE > 0.5$  and  $Pbias \leq \pm 15\%$  as suggested by Moriasi (2007) and Moriasi et al.

468

(2015). In addition, the simulated daily streamflow in the no-wetland and no wetlands-reservoir

469

scenarios both overestimated the high flows, especially those during the flood periods; during the low

470

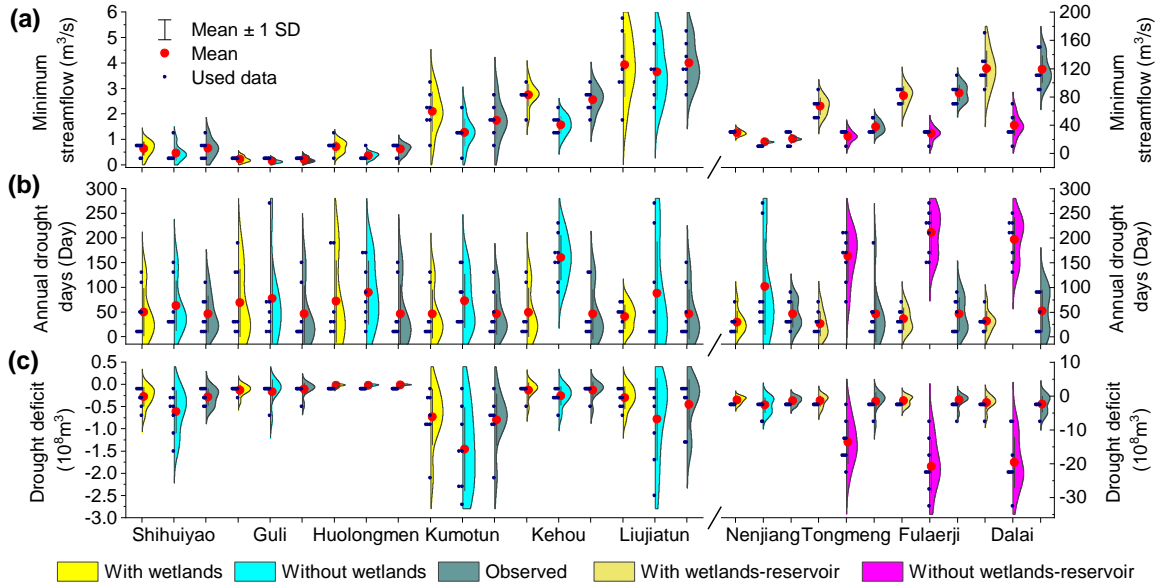
flow periods, the low flows were underestimated (Please refer to Fig. A1 in Supplementary materials).

471 Further, the simulated hydrographs under the wetland and wetlands-reservoir scenario were in much  
472 better agreement with the hydrographs of observed streamflow, especially during floods and the low-  
473 flow period (Please refer to Fig. A2 in Supplementary materials). These results indicate that inclusion  
474 of the wetlands and the operation of reservoirs can greatly improve model capacity to replicate basic  
475 hydrograph characteristics and capture hydrological extremes (e.g., high and low flows).

### 476 3.2 Model capacity to replicate flood and drought characteristics

477 The simulated annual minimum streamflow for the wetlands/wetlands-reservoir scenarios were, in  
478 general, slightly overestimated or approximately equivalent to the observations compared to the  
479 scenarios that did not include the wetlands/wetlands-reservoir (Fig. 3). However, the simulation results  
480 without wetlands clearly underestimated minimum streamflow, distinctly overestimated annual drought  
481 days and drought deficit compared to the simulation results for the scenario with wetlands at the ten  
482 hydrological stations. In addition, the simulated annual maximum peak flow, flood days and volume  
483 under the with/without wetland scenarios are, in general, approximately comparable to observations at  
484 the Guli, Kumotun, Kehou, Liujiatun and Nenjiang hydrological stations (Fig. A4). Specifically, for the  
485 upstream Nierji Reservoir, it is apparent that if wetlands are not considered, the number of annual flood  
486 days will be overestimated, whereas flood volume will be substantially underestimate at the  
487 Huoloengmen Station. For the lower reach of Nierji Reservoir, lack of integrating the wetlands and  
488 reservoir into the simulation can lead to a notable underestimation of annual flood days, and a substantial  
489 overestimation of the annual maximum peak flow and flood volume. These results demonstrate that  
490 integrating wetlands and the combination of wetlands and the reservoir into the model can help improve  
491 model performance with regards to flow during the calibration process, and enhances the model's  
492 capability of depicting streamflow processes as well as capturing flood and drought characteristics.

493



494

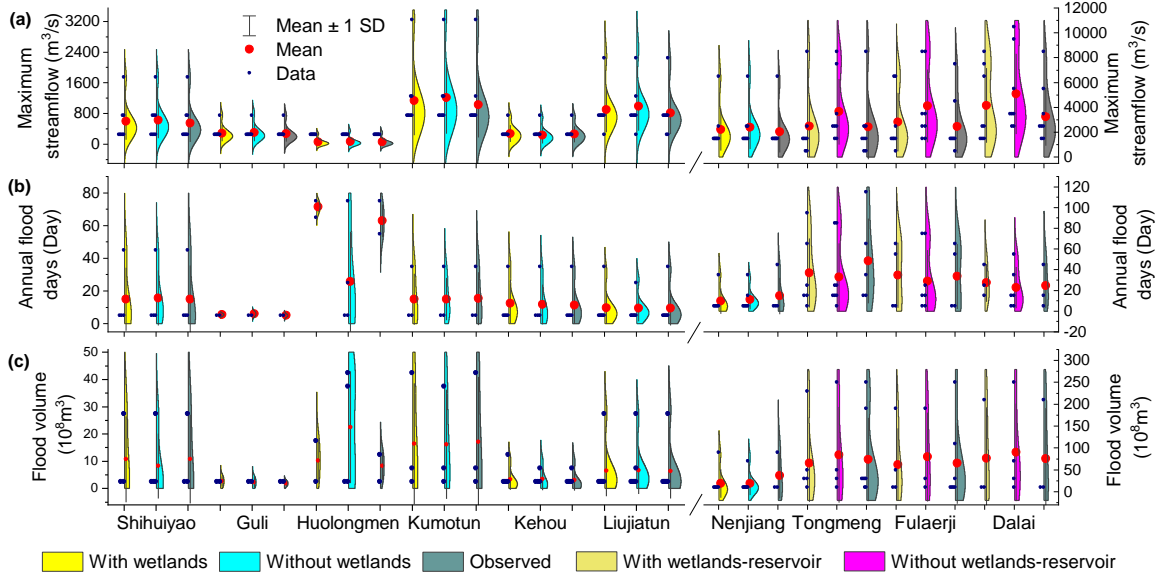
495

496

497

498

Figure. 3. Annual minimum streamflow, drought days and deficit derived from observed records and simulated streamflow at ten hydrological stations in the Nenjiang River Basin. The with and without wetlands/wetlands-reservoir refers to streamflow simulation based on the presence or absence of wetlands/wetlands-reservoir.



499

500 Figure 4. Annual maximum peak flow, flood days and volume derived from observed records and simulated  
 501 streamflow at ten hydrological stations in the Nenjiang River Basin. The with and without wetlands/wetlands-  
 502 reservoir refers to streamflow simulation based on the presence or absence of wetlands/wetlands-reservoir.

503

### 504 3.3 Projection of future floods

505 A comparison between historical and projected flood characteristics at the Nenjiang Station  
 506 (representing inclusion of wetlands into hydrological modeling) shows an overall increase in flood risks  
 507 in the upper NRB. The flood duration, peak flow, volume and flashiness generally exhibit larger  
 508 fluctuations in most of the scenarios (different SSPs and three periods as shown in Fig. A3 and Table  
 509 A1). In addition, the averaged increase in flood duration, peak flow, volume and flashiness ranges from  
 510 0.9 to 1.2%, from 16 to 33%, from 8 to 111% and from 26 to 55%, respectively (Fig.6). Specifically,  
 511 the extreme values of flood duration are much larger during the near future and end-century under the  
 512 SSP126 scenario, the end-century under the SSP370 scenario and the mid- and end-century under the  
 513 SSP585 scenario (Fig. 6a). Apart from a slight decrease during the near future and mid-century under  
 514 the SSP585 scenario, peak flow will increase through time in the SSP126, SSP370 and SSP585 scenarios  
 515 (Fig. 6b). Simultaneously, the flood volume will experience the greatest increase of 68% during the near  
 516 future under the SSP585 scenario, followed by a 22% increase during the mid-century under the SSP126  
 517 scenario (Fig. 6c). In terms of flashiness, the floods will be more severe under the constrains inherent

518 in the SSP126 and SSP585 scenarios and less severe given the conditions in the SSP370 scenario, as  
519 compared to the historical period (Fig. 6d).

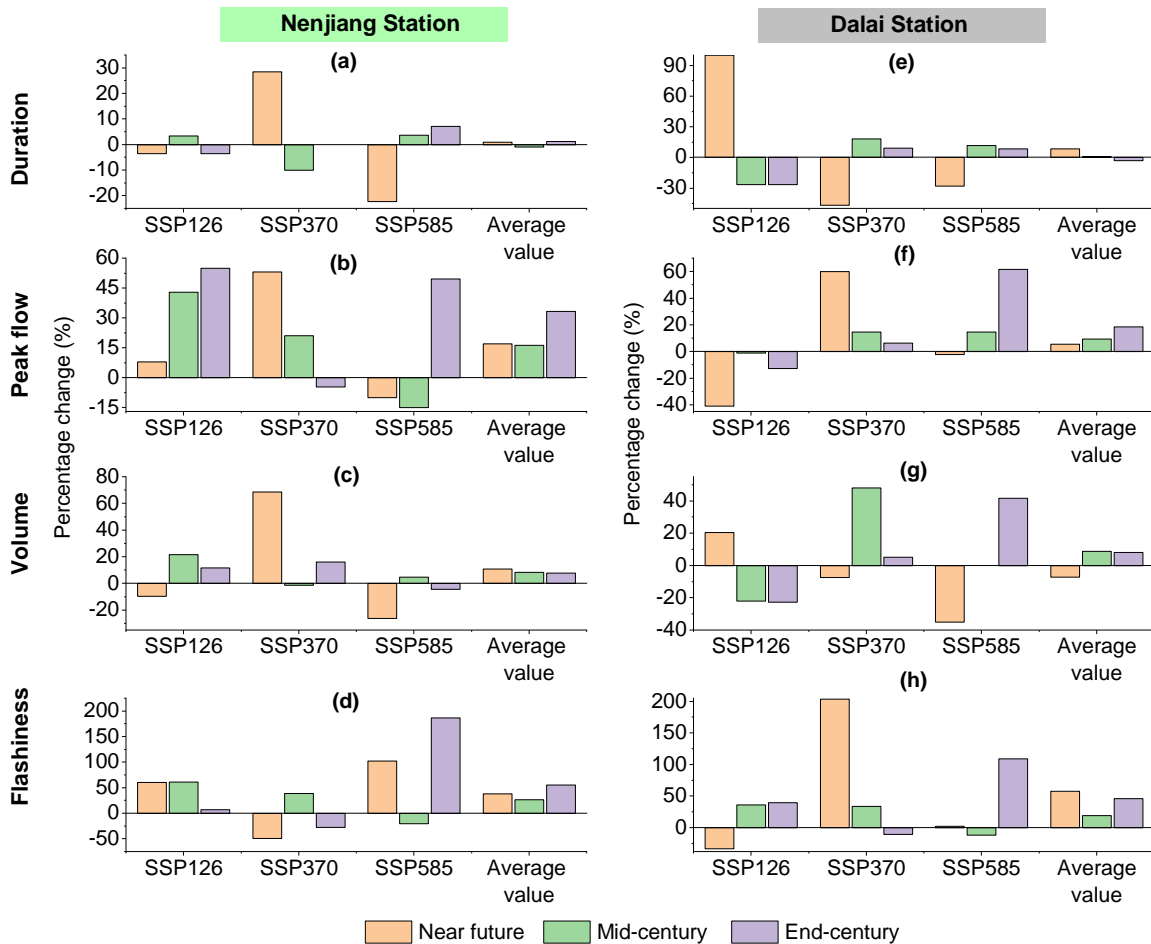
520 It should be noted that the flood duration, peak flow, volume and flashiness can decrease in the future,  
521 as compared to the historical period (Fig.6). For example, flood duration will slightly decrease during  
522 the near future and end-century under the SSP126 scenario, largely decrease during the near future under  
523 the SSP585 scenario, respectively. Under the SSP585 scenario, the flood peak flow will experience a  
524 decrease with the percentage change values of 15% during the mid-century and the volume will reduce  
525 26% during near future. In addition, future flood flashiness will be reduced by 49% and 28% in the near  
526 future and the end-century under the SSP370 scenario respectively, and by 21% at mid-century under  
527 the SSP585 scenario.

528 The changes in the historical and future flood duration, peak flow, volume and flashiness at the Dalai  
529 Station (representing inclusion of downstream wetlands and reservoir operation into hydrological  
530 modeling) is shown in Fig.A3 and Fig.4 e-h. Similar to the Nenjiang station, the flood duration, peak  
531 flow, volume and flashiness at the Dalai station also exhibit divergent change trends across different  
532 SSPs and three periods, as compared to the historical periods. Flood duration is projected to increase  
533 largely in the near-future period for the SSP126 scenario, both in the mid-century and end-century for  
534 the SSP370 scenario (Fig.6e). The peak flow will broadly decrease for the SSP126 scenario, and increase  
535 for the SSP370 and 585 scenarios (Fig.6f). Flood volume shows divergent change trends under the three  
536 SSPs (Fig.4g). For the SSP126 scenario, flood volume will grow in the near-future and diminish in the  
537 mid- and end-century. Flood volume will decrease in the near-future, increase in the mid-century, and  
538 increase slightly in the end-century under the SSP370 scenario. However, following an apparent  
539 reduction in the near-future, flood volume is anticipated to have no discernible change trend in the mid-  
540 century and a clear increasing trend in the end-century for the SSP585 scenarios. Flashiness will be  
541 reduced in the near future and will increase in the mid-century and end-century for the SSP126 scenario  
542 (Fig.6h). For the SSP370 scenario, flashiness will increase substantially with percentage changes of 204%  
543 in the near-future, Moreover, for the SSP585 scenario, flashiness will experience a considerable increase  
544 with percentage changes of 109% in the end-century respectively. In terms of the averaged percentage



545 change values, the peak flow and flood flashiness will overall increase; the flood volume will reduce in  
 546 the near future and rise in the mid-century and end-century; and flood duration will experience a slight  
 547 increase to a minor decrease.

548



549

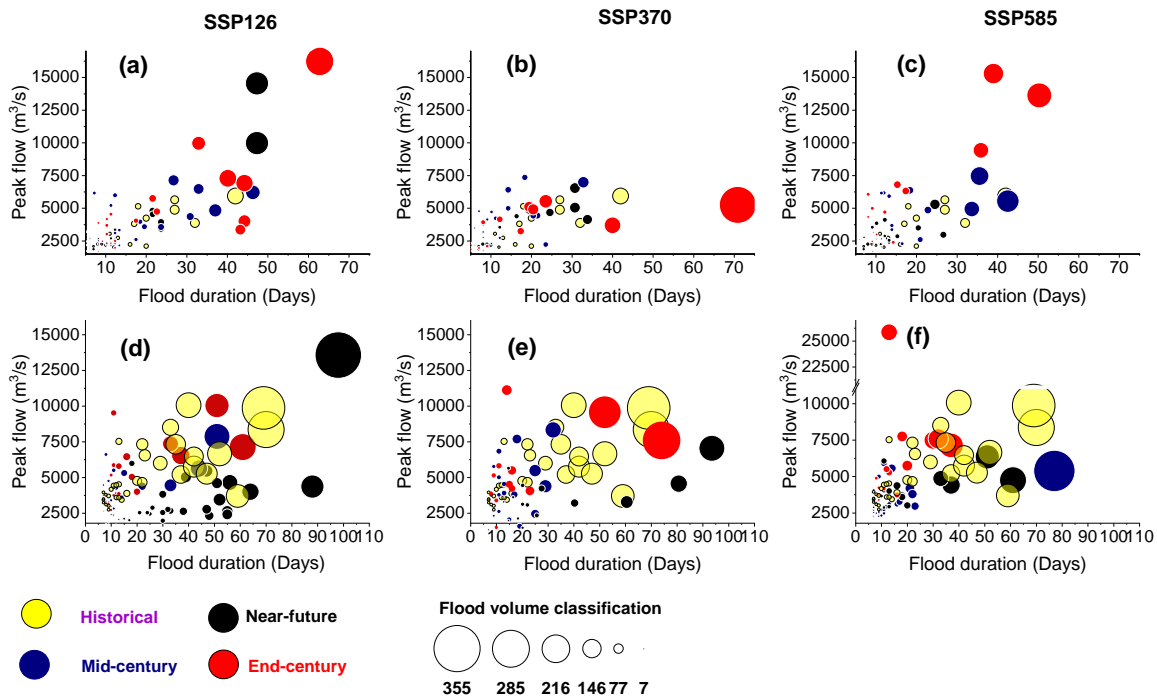
550 Figure 6. Projected percentage changes (relative to historical period during 1971-2020) in flood duration,  
 551 peak flow, volume and flashiness at the Nenjiang (the left column) and Dalai (the right column) Station. The  
 552 near-future, mid-century and end-century refer to the 2026-2050, 2051-2075 and 2076-2100 under the  
 553 Socioeconomic Pathways (SSP) 126, SSP370 and SSP585 scenarios. The average values were calculated  
 554 based on the projected percentage changes in the three SSP scenarios.

555

556 To further investigate flood risks in the NRB under future climate change, the flood duration-peak  
 557 flow-flow volume relationships at the Nenjiang and Dalai stations for the SSPs were compared to those

558 of the historical period and analyzed (Fig. 7a-c). Compared with historical flood risk, extreme flood  
 559 events with longer and larger volumes will occur more frequently at the Nenjiang Station for the SSP126  
 560 and SSP585 scenarios (Fig. 7a and 7c). It is noteworthy that the flood peak-volume-duration  
 561 relationships between the historical period and SSP370 scenario are approximate equal, with the  
 562 exception that longer duration and larger volume floods will occur during the end-century period (Fig.  
 563 5b). In addition, extreme flood events will occur mainly in the near-future for the SSP126 scenario and  
 564 during the mid- and end-century for the SSP585 scenario. Moreover, for the SSP370 and SSP585  
 565 scenarios, floods will become shorter in duration, and possess a lower peak flow and flood volume in  
 566 the near-future. Thus, the upper NRB will experience more severe flood events to a large extent under  
 567 most future climate change scenarios.

568



569

570 **Figure 7.** Historical and projected flood duration-peak flow-volume relationships at the Nenjiang (the  
 571 first row) and Dalai (the second row) Station. The historical period refers to 1971-2020 and the near-  
 572 future, mid-century and end-century refer to the 2026-2050, 2051-2075 and 2076-2100 under the  
 573 Socioeconomic Pathways (SSP) 126 (the first column), SSP370 (the second column) and SSP585 (the

574 third column) scenarios.

575

576 The duration-peak flow-volume relationships of extreme flood events under future climate change  
577 scenarios are closer to those of the historical period at the Dalai Station than at the Nenjiang Station  
578 (Fig. 7d-f). For the three future SSPs, the flood events with longer duration, higher peak flows or larger  
579 volume than the historical period will occur infrequently, and the duration, flood volume and peak  
580 flow of the other shorter and lower magnitude flood events will generally be attenuated. However, very  
581 extreme flood events are projected to occur in the near-future under the conditions of scenario SSP126  
582 (Fig. 7d). Likewise, future climate change under the SSP370 scenario and 585 scenarios are projected  
583 to result in longer flood events in the near-future and mid-century, respectively (Fig. 7e and 7f).  
584 Therefore, the future flood risk can be effectively attenuated to a great extent by the combined influence  
585 of wetlands and reservoir. However, extreme floods will still occur in the future.

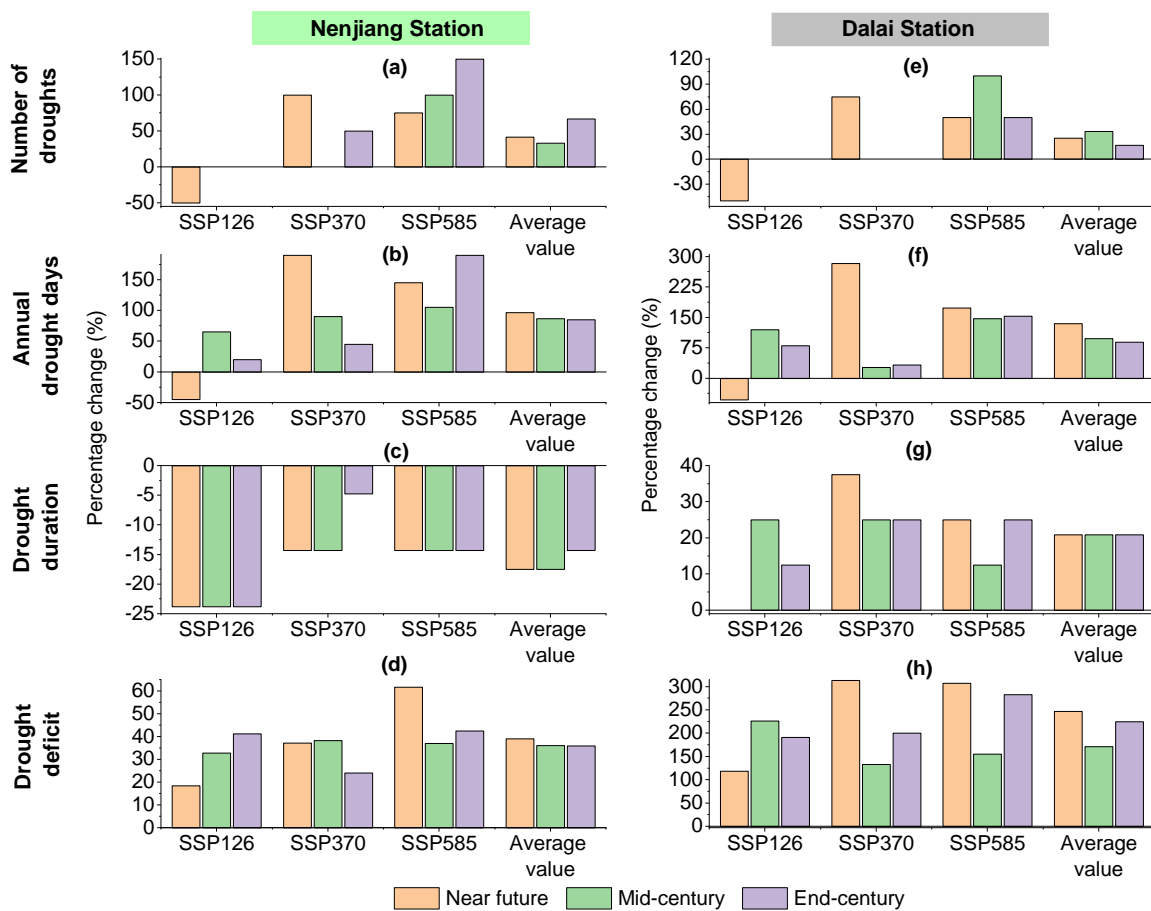
#### 586 3.4. Prediction of future hydrological droughts

587 The comparison between historical and projected hydrological drought indices shows that the risks  
588 of hydrological droughts will be increased to some extent under future climate change for both Nenjiang  
589 and Dalai stations. Specifically, in addition to a reduction in the number of droughts and annual drought  
590 days in the near future for the SSP126 scenario, the number of droughts (Fig. 8a and 8e), annual drought  
591 days (Fig. 8b and 8f) and drought deficit (Fig. 8d and 8h) will overall increase in other periods for three  
592 scenarios (Figure A4 and Table A2). It is clear that the number of droughts will be equivalent to the  
593 historical period in the mid-century and end-century for the SSP126 scenario and in the mid-century for  
594 the SSP585 scenario. For all other scenarios, the number of droughts will increase. In terms of the mean  
595 percentage change values, there is a general trend towards an increase in the number of droughts and  
596 annual drought days, which indicate that future drought events will be more frequent and there will be  
597 more days per year affected by drought. The predicted extreme values show that the future duration of  
598 drought at Nenjiang station may be shorter than the historical period, but the degree of shortening  
599 presented in different SSP scenarios varies (Fig. 8c and 8g). For the Dalai station, the longest drought  
600 durations would all exceed historical extremes in the end-century for the SSP126 and SSP585 scenario,

601 and in the near future for the SSP370 scenario. The percentage change values display that drought  
 602 duration will be reduced at the Nenjiang station and will be extended at the Dalai station for all the SSP  
 603 scenarios. Drought deficit at the Dalai station will increase by 39%, 36% and 36% and in the near future,  
 604 mid-century and end-century. For the Dalai station, drought deficit will increase further in the three  
 605 periods with 39%, 36% and 36%, respectively.

606 A comparison of the percentage change values between the Nenjiang and Dalai stations shows that,  
 607 apart from a reduction of the number of drought events, the risk of drought to be experienced at Dalai  
 608 is considerably stronger than at Nenjiang. Specifically, the percentage change in the annual drought  
 609 days, drought duration and deficit will increase from 85-97% to 89-134%, from -17- -17% to 21%, and  
 610 from 36-39% to 171-247%, respectively.

611



612

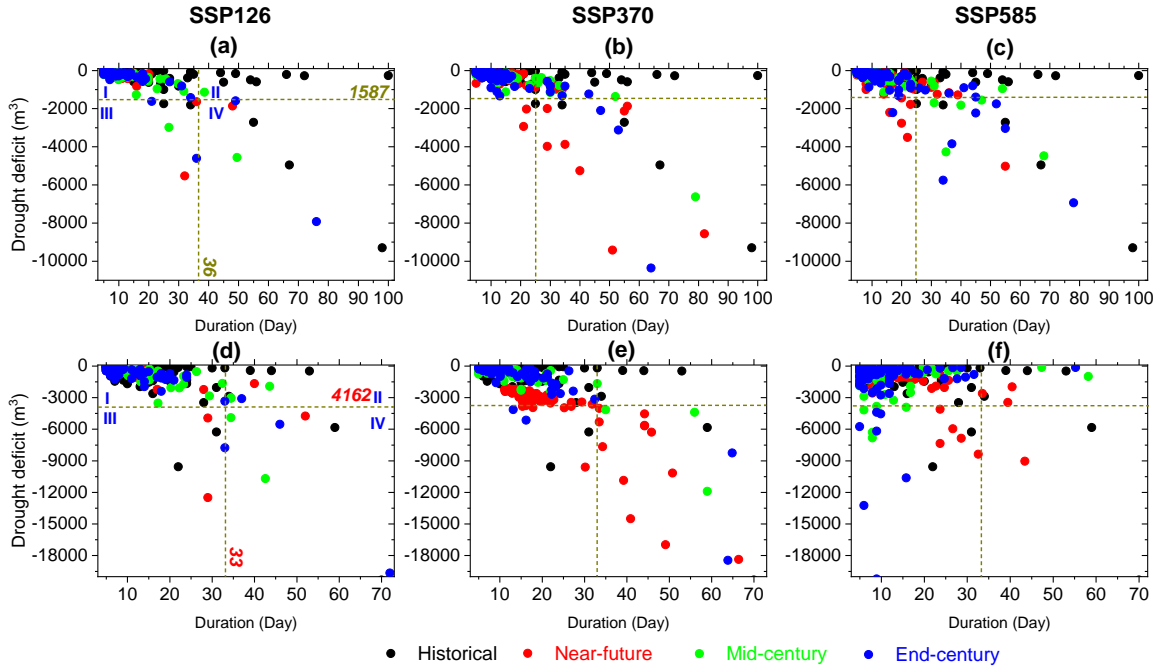
613 Figure 8. Projected percentage changes (relative to historical period during 1971-2020) in hydrological

614 drought characteristics at the Nenjiang (the left column) and Dalai (the right column) Station. The near-future,  
615 mid-century and end-century refer to the 2026-2050, 2051-2075 and 2076-2100 under the Socioeconomic  
616 Pathways (SSP) 126, SSP370 and SSP585 scenarios. The average values were calculated based on the  
617 projected percentage changes in the three SSP scenarios.

618

619 To further analyze the temporal evolution of droughts in the Nenjiang River Basin under future  
620 climate change, drought events were classified into four types in terms of duration and deficit, i.e., short-  
621 term light droughts, long-term light droughts, short-term severe droughts, and long-term severe droughts  
622 (see Fig. 9 for details). This four-part classification was then used to compare and analyze the changes  
623 in the temporal characteristics of drought events under the different SSP scenarios. Similar to the  
624 drought characteristics during the historic historical period, the majority of drought events for the  
625 SSP126, SSP370 and SSP585 scenarios are short-term light droughts (Fig. 9a-c), i.e., the upper NRB  
626 will still be dominated by short-term light droughts under future climate change. However, these  
627 droughts will be slightly aggravated and marginally longer. In addition, long-term light droughts will  
628 occur rarely under the conditions inherent in scenarios SSP126 (Fig. 9a) and SSP370 (Fig. 9b), and  
629 occur relative frequently in the SSP585 scenario (Fig. 9c). However, compared with the historical period,  
630 the overall number of long-term light droughts will largely decrease, but the deficit will increase slightly  
631 under future climate change. In addition, short-term severe droughts will increase substantially, along  
632 with their deficit. The number of long-term severe droughts for the SSP126 scenario is approximately  
633 the same as in the past, but the duration will be substantially reduced. For scenarios SSP370 and SSP585,  
634 the number of long-term severe droughts will increase more than during the historical period, but the  
635 duration will be markedly less, and the deficit will be reduced to some extent. In terms of the different  
636 the sub-periods, severe droughts in the upper NRB will be more severe during the near-future and end-  
637 century periods, and relatively less severe in the mid-century period in comparison to the historical  
638 period. However, overall, the droughts will be of shorter duration and characterized by an increased  
639 deficit under future climates.

640



641

642 **Figure 9.** Historical and projected duration-deficit relationship of each hydrological droughts at the Nenjiang  
 643 (the first row) and Dalai (the second row) Station. The historical period refers to 1971-2020 and the near-  
 644 future, mid-century and end-century refer to the 2026-2050, 2051-2075 and 2076-2100 under the  
 645 Socioeconomic Pathways (SSP) 126 (the first column), SSP370 (the second column) and SSP585 (the  
 646 third column). The dark yellow lines in the horizontal and vertical directions refer the 95% threshold lines  
 647 for drought deficit and duration values, respectively. I, II, III and IV refer to short-term light droughts, long-  
 648 term light droughts, short-term severe droughts, and long-term severe droughts, respectively.

649

650 Droughts brought about by future climate change at the Dalai Station located along the lower reaches  
 651 of the NRB will continue to be dominated by short-term slight droughts (Fig. 9d-f). For the SSP126  
 652 scenario, the duration and deficit of the short-term slight droughts will be approximately the same as  
 653 those during historical times (Fig. 9d). However, the duration and deficit of short-term slight droughts  
 654 will increase given the conditions specified in the SSP370 (Fig. 9e) and SSP585 (Fig. 9f) scenarios. The  
 655 duration of short-term slight droughts will increase the most for scenario SSP370. In addition, under all  
 656 three SSP scenarios, long-term slight droughts will, in general, be reduced. In fact, under the SSP370  
 657 scenario, long-term slight droughts will not occur. The number of short-term severe droughts will

658 generally tend to increase, with the most pronounced increase under the SSP585 scenario, followed by  
659 the SSP370 scenario. A slight increase will occur under the SSP126 scenario. However, long-term  
660 severe droughts will increase substantially under the SSP126 and SSP370 scenarios. In particular, under  
661 the SSP370 scenario, the duration of long-term severe droughts will be exceptionally prolonged, and  
662 the severity will be extraordinarily increased, indicating that the risk of droughts of long duration and  
663 with a severe deficit will climb abnormally in some year. For example, under the conditions set by the  
664 SSP370 scenario, the deficit of long-term severe droughts will reach -18,169 m<sup>3</sup> and -18,457 m<sup>3</sup> during  
665 the near-future and end-century periods. For the SSP585 scenario, long-term severe drought will occur  
666 only once in the near-future, which is equivalent to the historical period. These results indicate that the  
667 risk of future hydrologic droughts along the lower NRB will further increase even under the combined  
668 influence of reservoirs and wetlands.

669

#### 670 **4. Discussion**

671 4.1. Integrating wetlands and reservoir operation into basin hydrologic modeling and basin water  
672 management

673 A series of studies have shown that the simulation and prediction of floods and droughts faces many  
674 challenges, such as the scarcity of hydrometeorological driven data (Foulon et al., 2018), model errors  
675 (Golden et al., 2021; Smakhtin, 2001; Staudinger et al., 2011) and anthropogenic disturbances (e.g.,  
676 reservoir operation) (Brunner, 2021; Brunner et al., 2021). In this study, we developed a spatially  
677 explicit hydrological model that considers wetland hydrological processes and reservoir operations  
678 through coupling a distributed hydrological modeling platform with wetland modules and reservoir  
679 simulation algorithms. We found that coupling wetland alone or coupling wetlands and reservoir with  
680 hydrological model can improve model calibration results and model performance of capturing flood  
681 and drought characteristics in a large river basin. Such model performance improvement can provide  
682 important information for developing downstream water resources management. Previous studies have  
683 shown that climate change is further exacerbating the risk of hydrological extremes, leading to an

684 expanding of flood and drought affected area (Diffenbaugh et al., 2015; e.g., Hirabayashi et al., 2013;  
685 Wang et al., 2021), which increase the complexity of accurate prediction and the challenge for effective  
686 mitigation. Give that, projecting flood and drought risks in response to a changing climate requires  
687 robust hydrologic models that take into account the important factors within a watershed that can largely  
688 influence basin hydrological processes (Golden et al., 2021). Therefore, in basins that coexist with high-  
689 coverage wetlands and multiple reservoirs, it is necessary to integrate wetlands and reservoir operation  
690 into basin hydrological simulation, thus providing practical support for extreme hydrological risk  
691 mitigation and water resource management under a changing climate.

692 Although our developed framework demonstrates good modeling results, uncertainties could exist in  
693 the assessment. Aspects such as the accuracy and error of the input data (Lobligeois et al., 2014), the  
694 choice of the objective function (Fowler et al., 2018), the length of the period considered during  
695 calibration (Arsenault et al., 2018), and the model structure (Melsen et al., 2019) can all affect the  
696 performance of a model to replicate streamflow, thus impacting flood and drought predictions and water  
697 management under future climate change. In addition, due to a lack of wetlands water balance  
698 monitoring data, this study only used river station data (which only considered the cumulative  
699 hydrologic effect of upstream wetlands) for model calibration. Therefore, there are ongoing efforts to  
700 obtain sufficient observations on wetland area dynamics and evapotranspiration, water depth and  
701 volume, soil water content and actual observations to better calibrate/validate watershed hydrological  
702 models, which are expected to better provide key parameters for further improving the model's capacity  
703 to capture flood and drought patterns and better serve basin water management. In addition, the several  
704 SPPs employed to drive the simulation framework, including SSP126, SSP370, and SSP585 scenarios,  
705 can introduce uncertainty into future flood and drought risk projections. Because of the internal  
706 variability and uncertainties inherent in the existing climate models (Qing et al., 2020; Martel et al.,  
707 2022), the projection findings under different scenarios were inconsistent, creating a challenge for pro-  
708 active management and mitigation decisions. Despite the climate models' recognized flaws and  
709 uncertainties, the general concordance between models and observations over many regions suggests  
710 some improved confidence in their utility for understanding and mitigating future drought and climate



711 change (Cook et al., 2020). Furthermore, several reservoirs and a large number of wetlands are spread  
712 throughout the NRB's tributaries (Meng et al., 2019), which individually and together play an essential  
713 role in drought and flood risk reduction. We only investigated the impacts of mainstream reservoirs and  
714 wetlands on drought and flood risk due to a lack of sub-basin reservoir operation observations. As a  
715 result, future integrated wetland-reservoir simulations of all mainstream and tributaries for flood-  
716 drought risk assessment will be done based on further data collection. Since the Nierji reservoir is the  
717 largest in the NRB and has the most influence on the mainstream runoff regime, our findings based on  
718 the simulation of Nierji reservoir and wetlands can give new insights into future floods and droughts, as  
719 well as provide important support for future hydrological extremes adaptation.

#### 720 4.2. The combining mitigation efficiency of wetlands and reservoir operation

721 The relative changes (compared with historical periods) of future flood and drought indices (Fig. 6  
722 and 8), duration-peak flow-volume relationships (Fig. 7) and duration-deficit relationship (Fig. 9) differ  
723 between the Nenjiang and Dalai stations under the same SSP scenario or in the same period, indicating  
724 that reservoirs and downstream wetlands can modify the continuous propagation of upstream flood and  
725 hydrological drought risks to the downstream. First, reservoirs and downstream wetlands can help to  
726 reduce the risks of future floods and droughts to some extent, namely partially reduce flood peak flow  
727 and flashiness, and decrease the number of droughts, annual drought days and drought deficit. Second,  
728 reservoirs and downstream wetlands cannot completely eliminate flood and drought risks. Because the  
729 flood duration and volume will overall increase at the Dalai station, especially that the extreme floods  
730 will be more frequent in the future (Fig.7). Further, in addition to the number of droughts, the percentage  
731 change values of the annual drought days, drought duration and deficit relative change at the Dalai  
732 Station are greater than those of Nenjiang Station (Fig.8). This imply that the mitigation effects on  
733 hydrological droughts is minimal. Such findings suggest that future climate change will lead to an  
734 increase in the risk of hydrologic failure of existing reservoir and wetlands, thus posing large challenges  
735 for future socio-and eco-hydrological systems in the downstream NRB.

736 Wetlands are typically viewed as green infrastructures and reservoirs are generally regarded as  
737 important gray infrastructures. Although our study showed that the combining of reservoirs and

738 wetlands does not completely eliminate the risk of future hydrological extremes, they continue to play  
739 an important role that cannot be ignored. The reservoir's inherent constraints are one factor contributing  
740 to this likelihood of hydrological failure. This is because reservoirs only control floods and droughts  
741 that occur downstream of them, limiting their effects to the regional scale (Brunner, 2021). The  
742 regulation becomes less effective with distance increased due to "dilutions" effect caused by inflows  
743 from downstream tributaries (Guo et al., 2012). Reservoirs cannot, however, play a considerable role in  
744 basins where tributaries exist downstream, particularly those sub-basins prone to drought and flooding.  
745 From these perspectives, widely distributed wetlands can provide a complementary and vital function  
746 by providing biological function and hydrological regulation in regions where reservoirs are unable to  
747 have an impact. On the other hand, the limited capacity of existing wetlands to regulate hydrology  
748 increases the risk of hydrological failure to some extent. This is because, compared with the historical  
749 period, the existing wetlands in the NRB have been seriously degraded, such as the weakening of the  
750 connectivity between riparian wetlands and the river channel, and the increased fragmentation of  
751 wetlands, among other changes (Chen et al., 2021). These degraded wetlands cannot play an effective  
752 role in mitigating floods and droughts under future climate change.

753

#### 754 4.3. Implications for flood and drought risk management under climate change

755 This modeling study predicts higher flood and drought risks in the NRB under the combined influence  
756 of wetlands and reservoirs. This could impose a great challenge to the operation of the Nierji Reservoir  
757 dam, i.e., to its effective operation for flood mitigation and drought alleviation. To curb the flood and  
758 drought risks caused by future climate change in the NRB, it is urgent to improve the water regulation  
759 capacity of the lower NRB. Although the Nierji Reservoir, as previously argued, plays an important role  
760 in reducing floods and droughts, the potential for extreme hydrological events in the future necessitate  
761 the application of various combinations of measures with different scales of implementation (i.e., hybrid  
762 measures). We insist that the first remedial measure to be undertaken should be the implementation of  
763 wetland restoration and protection projects, because studies have demonstrated that wetland coverage  
764 and their spatial pattern can affect both basin physical conditions and human decision-making attitudes

765 toward risk (Gómez-Baggethun et al., 2019; Javaheri and Babbar-Sebens, 2014; Martinez-Martinez et  
766 al., 2014; Zedler and Kercher, 2005). Given that the spatial location of wetlands within a river basin is  
767 also important in determining the efficiency of their mitigation services (Gourevitch et al., 2020; Li et  
768 al., 2021; Zhang and Song, 2014), optimization of wetland spatial patterns should be considered and can  
769 be carried out to further enhance the role of wetlands in flood and drought defense.

770 In our view, the second important remedial measure that should be implemented is to improve the  
771 existing reservoir operation schemes based on accurate hydrological forecasting. This requires, on one  
772 hand, coupling of wetlands with hydrological processes and models to improve the simulation accuracy  
773 of the upstream incoming water (i.e., runoff from the Nenjiang Station) to provide scientific support for  
774 reservoir operation decisions. Concomitantly, it is necessary to modify the existing schemes for optimal  
775 reservoir operation to improve the system's capacity to deal with extreme flood and drought risks.  
776 Because the percentage increase in flood (Fig. 6) and drought indicators (Fig. 8) demonstrated that the  
777 existing reservoir operation schemes are not effective in mitigating the risks associated with future  
778 climate change-induced floods and droughts. Therefore, we need to re-examine and evaluate the flood  
779 and drought risks in the NRB under future climate change and propose optimal operation schemes that  
780 can maximize the reduction of flood and drought risks by the Nierji Reservoir. Traditionally, the water  
781 level of a reservoir should be maintained at the designed flood limited water level during the flood  
782 season, which does not consider river flow forecast. (Ding et al., 2015) analyzed a concept that provides  
783 a dynamic control of the maximum allowed water level during the flood season, for the Nierji Reservoir  
784 dam. A reasonable approach to tackle this issue could be to considerate forecast uncertainty and  
785 acceptable flood risk to minimize the total loss caused by flood and drought. Further modeling studies  
786 with multi-objective optimization algorithm can help identify an optimum reservoir operation for best  
787 economic and ecological outcomes.

## 788 **5. Conclusions**

789 This study projected future flood and drought risks by considering the combined impacts of wetlands  
790 and reservoirs. To achieve this, we developed a hydrological modeling framework coupled wetlands

791 and reservoir operations and then applied it in a case study involving a 297,000-km<sup>2</sup> large river basin in  
792 northeast China. With this framework, we found that coupling wetlands and reservoir operations can  
793 slightly increase model calibration results and efficiently improve model capacity to capture both flood  
794 and hydrological drought characteristics in a river basin. The upper NRB will experience more severe  
795 flood and hydrological droughts and can impose a great challenge to the effective operation of  
796 downstream reservoir under the predicted future climate change scenarios. The risk of future floods and  
797 hydrologic droughts along the lower NRB will further increase even under the combined influence of  
798 reservoirs and wetlands. These results demonstrated that the risk of floods and droughts will overall  
799 increase further under future climate change even under the combined influence of reservoirs and  
800 wetlands, showing the urgency to implement wetland restoration and develop accurate forecasting  
801 systems. To fully understand how wetland and reservoir operations may be influential and maintain an  
802 acceptable level of risk, it is therefore necessary to consider an optimization of wetland spatial patterns  
803 and reservoir operations simultaneously, thus achieving a collaborative optimization management to  
804 maximum basin resilience to floods and hydrological droughts. Further, the effects of combining NBS  
805 (e.g., wetlands) with traditional engineering solutions (e.g., reservoir) should both be useful and  
806 necessary in the future for management decisions.

807

#### 808 **Data Availability**

809 The data used in this study are openly available for research purposes. The five GCM outputs (GFDL-  
810 ESM4, IPSL-CM6A-LR, MPI-ESM1-2-HR, MRI-ESM2-0, and UKESM1-0-L) used in this study are  
811 publically available and were provided by the Inter-Sectoral Impact Model Intercomparison Project  
812 (ISIMIP) (<https://esg.pik-potsdam.de/search/isimip/>). The CMhyd software is available at  
813 <https://swat.tamu.edu/software/cmhyd>. The land-use/land-cover types, soil texture, and digital elevation  
814 model for China can be downloaded from <https://www.resdc.cn/>. Data from the 88 weather stations  
815 administered by National Meteorological Information Centre of China can be download at  
816 <http://data.cma.cn>.

817

818 **Author contribution**

819 **Yanfeng Wu:** Conceptualization, Writing, Data analysis, Methodology, Software. **Jingxuan Sun:**  
820 Formal analysis, Investigation, Data analysis and Plotting. **Boting Hu:** Software, Visualization, Data  
821 analysis. **Y. Jun Xu:** Writing - review & editing. **Alain N. Rousseau:** Writing - review & editing.  
822 **Guangxin Zhang:** Conceptualization, Supervision, review & editing.

823

824 **Competing interests**

825 The authors declare that they have no known competing financial interests or personal relationships  
826 that could have appeared to influence the work reported in this paper.

827

828 **Acknowledgments**

829 We are grateful to Jan Seibert for his valuable comments on the manuscript. The authors express their  
830 gratitude to the three anonymous reviewers for their constructive comments and suggestions that have  
831 helped improve the paper. We thank Anna Feist-Polner, Lorena Grabowski, Polina Shvedko and Sarah  
832 Buchmann for their efforts in the processing of the manuscript.

833

834

835 **Financial support**

836 This work was supported by the National Natural Science Foundation of China (42101051), the  
837 Postdoctoral Science Foundation of China (2021M693155), the Strategic Priority Research Program of  
838 the Chinese Academy of Sciences, China (XDA28020501, XDA28020105), and The National Key  
839 Research and Development Program of China (2021YFC3200203). During preparation of this  
840 manuscript, YJX received a grant from U.S. Department of Agriculture Hatch Fund (project number,

841 LAB94459).

842

843

844

845

846

847

848

849 **References**

850 Ahlén, I. et al., 2020. Wetlandscape size thresholds for ecosystem service delivery: Evidence from the  
851 Norrström drainage basin, Sweden. *Science of The Total Environment*, 704: 135452.

852 Åhlén, I., Thorslund, J., Hambäck, P., Destouni, G. and Jarsjö, J., 2022. Wetland position in the landscape:  
853 Impact on water storage and flood buffering. *Ecohydrology*, 15(7):e2458.

854 Alves, A., Gersonius, B., Kapelan, Z., Vojinovic, Z. and Sanchez, A., 2019. Assessing the Co-Benefits of  
855 green-blue-grey infrastructure for sustainable urban flood risk management. *Journal of Environmental*  
856 *Management*, 239: 244-254.

857 Anderson, C.C. and Renaud, F.G., 2021. A review of public acceptance of nature-based solutions: The  
858 ‘why’ , ‘when’ , and ‘how’ of success for disaster risk reduction measures. *Ambio*, 50(8): 1552-1573.

859 Arsenault, R., Brissette, F. and Martel, J., 2018. The hazards of split-sample validation in hydrological model  
860 calibration. *Journal of Hydrology*, 566: 346-362.

861 Beven, K., 1981. Kinematic subsurface stormflow. *Water Resources Research*, 17(5): 1419-1424.

862 Bosshard, T., Kotlarski, S., Ewen, T. and Schär, C., 2011. Spectral representation of the annual cycle in the  
863 climate change signal. *Hydrology and Earth System Sciences*, 15(9): 2777-2788.

864 Bouda, M. et al., 2014. Implementation of an automatic calibration procedure for HYDROTEL based on  
865 prior OAT sensitivity and complementary identifiability analysis. *Hydrological Processes*, 28(12): 3947-  
866 3961.

867 Bouda, M., Rousseau, A.N., Konan, B., Gagnon, P. and Gumiere, S.J., 2012. Bayesian Uncertainty Analysis  
868 of the Distributed Hydrological Model HYDROTEL. *Journal of Hydrologic Engineering*, 17(9): 1021-1032.

869 Boulange, J., Hanasaki, N., Yamazaki, D. and Pokhrel, Y., 2021. Role of dams in reducing global flood  
870 exposure under climate change. *Nature Communications*, 12(1).

871 Brunner, M.I., 2021. Reservoir regulation affects droughts and floods at local and regional scales.  
872 *Environmental Research Letters*, 16(12): 124016.

873 Brunner, M.I., Slater, L., Tallaksen, L.M. and Clark, M., 2021. Challenges in modeling and predicting floods  
874 and droughts: A review. *WIREs Water*, 8(3).

875 Cammalleri, C., Vogt, J. and Salamon, P., 2017. Development of an operational low-flow index for  
876 hydrological drought monitoring over Europe. *Hydrological sciences journal*, 62(3): 346-358.

877 Casal-Campos, A., Fu, G., Butler, D. and Moore, A., 2015. An Integrated Environmental Assessment of  
878 Green and Gray Infrastructure Strategies for Robust Decision Making. *Environmental Science & Technology*,  
879 49(14): 8307-8314.

880 Chen, L., Wu, Y., Xu, Y.J. and Guangxin, Z., 2021. Alteration of flood pulses by damming the Nenjiang  
881 River, China - Implication for the need to identify a hydrograph-based inundation threshold for protecting  
882 floodplain wetlands. *Ecological Indicators*, 124: 107406.

883 Cheng, C., Brabec, E., Yang, Y. and Ryan, R., 2013. Rethinking stormwater management in a changing world:  
884 Effects of detention for flooding hazard mitigation under climate change scenarios in the Charles River  
885 Watershed, *Proceedings of 2013 CELA Conference*, Austin, Texas, pp. 27-30.

886 Chiang, F., Mazdiyasn, O. and AghaKouchak, A., 2021. Evidence of anthropogenic impacts on global  
887 drought frequency, duration, and intensity. *Nature Communications*, 12(1).

888 Dang, T.D., Chowdhury, A.F.M.K. and Galelli, S., 2020. On the representation of water reservoir storage  
889 and operations in large-scale hydrological models: implications on model parameterization and climate  
890 change impact assessments. *Hydrology and Earth System Sciences*, 24(1): 397-416.

891 Diffenbaugh, N.S., Swain, D.L. and Touma, D., 2015. Anthropogenic warming has increased drought risk in  
892 California. *Proceedings of the National Academy of Sciences*, 112(13): 3931-3936.

893 Ding, W. et al., 2015. An analytical framework for flood water conservation considering forecast uncertainty  
894 and acceptable risk. *Water Resources Research*, 51(6): 4702-4726.

895 Dobson, B., Wagener, T. and Pianosi, F., 2019. An argument-driven classification and comparison of  
896 reservoir operation optimization methods. *Advances in Water Resources*, 128: 74-86.

897 Eriyagama, N., Smakhtin, V. and Udamulla, L., 2020. How much artificial surface storage is acceptable in a  
898 river basin and where should it be located: A review. *Earth-Science Reviews*, 208: 103294.

899 Evenson, G.R. et al., 2018. A watershed-scale model for depressional wetland-rich landscapes. *Journal of*  
900 *Hydrology X*, 1: 100002.

901 Evenson, G.R., Golden, H.E., Lane, C.R. and D Amico, E., 2015. Geographically isolated wetlands and  
902 watershed hydrology: A modified model analysis. *Journal of Hydrology*, 529: 240-256.

903 Evenson, G.R., Golden, H.E., Lane, C.R. and D'Amico, E., 2016. An improved representation of  
904 geographically isolated wetlands in a watershed-scale hydrologic model. *Hydrological Processes*, 30(22):  
905 4168-4184.

906 Fleig, A.K., Tallaksen, L.M., Hisdal, H. and Demuth, S., 2006. A global evaluation of streamflow drought  
907 characteristics. *Hydrol. Earth Syst. Sci.*, 10(4): 535-552.

908 Fortin, J. et al., 2001. Distributed Watershed Model Compatible with Remote Sensing and GIS Data. I:  
909 Description of Model. *Journal of Hydrologic Engineering*, 6(2): 91-99.

910 Fossey, M., Rousseau, A.N., Bensalma, F., Savary, S. and Royer, A., 2015a. Integrating isolated and riparian  
911 wetland modules in the PHYSITEL/HYDROTEL modelling platform: model performance and diagnosis.  
912 *Hydrological Processes*, 29(22): 4683-4702.

913 Fossey, M., Rousseau, A.N., Bensalma, F., Savary, S. and Royer, A., 2015b. Integrating isolated and riparian  
914 wetland modules in the PHYSITEL/HYDROTEL modelling platform: model performance and diagnosis.  
915 *Hydrological Processes*, 29(22): 4683-4702.

916 Foulon, É., Rousseau, A.N. and Gagnon, P., 2018. Development of a methodology to assess future trends in  
917 low flows at the watershed scale using solely climate data. *Journal of Hydrology*, 557: 774-790.

918 Fowler, K., Peel, M., Western, A. and Zhang, L., 2018. Improved Rainfall - Runoff Calibration for Drying  
919 Climate: Choice of Objective Function. *Water Resources Research*, 54(5): 3392-3408.

920 Garcia, F., Folton, N. and Oudin, L., 2017. Which objective function to calibrate rainfall - runoff models for  
921 low-flow index simulations? *Hydrological Sciences Journal*, 62(7): 1149-1166.

922 Golden, H.E., Lane, C.R., Rajib, A. and Wu, Q., 2021. Improving global flood and drought predictions:  
923 integrating non-floodplain wetlands into watershed hydrologic models. *Environmental Research Letters*,  
924 16(9): 091002.



925 Gómez-Baggethun, E. et al., 2019. Changes in ecosystem services from wetland loss and restoration: An  
926 ecosystem assessment of the Danube Delta (1960 – 2010). *Ecosystem Services*, 39: 100965.

927 Gourevitch, J.D. et al., 2020. Spatial targeting of floodplain restoration to equitably mitigate flood risk.  
928 *Global Environmental Change*, 61: 102050.

929 Gulbin, S., Kirilenko, A.P., Kharel, G. and Zhang, X., 2019. Wetland loss impact on long term flood risks in  
930 a closed watershed. *Environmental Science & Policy*, 94: 112-122.

931 Güneralp, B., Güneralp, O. and Liu, Y., 2015. Changing global patterns of urban exposure to flood and  
932 drought hazards. *Global Environmental Change*, 31: 217-225.

933 Guo, H., Hu, Q., Zhang, Q. and Feng, S., 2012. Effects of the Three Gorges Dam on Yangtze River flow and  
934 river interaction with Poyang Lake, China: 2003-2008. *Journal of Hydrology*, 416: 19-27.

935 Gupta, H.V., Kling, H., Yilmaz, K.K. and Martinez, G.F., 2009. Decomposition of the mean squared error  
936 and NSE performance criteria: Implications for improving hydrological modelling. *Journal of Hydrology*,  
937 377(1-2): 80-91.

938 Hagemann, S. and Jacob, D., 2007. Gradient in the climate change signal of European discharge predicted  
939 by a multi-model ensemble. *Climatic Change*, 81(S1): 309-327.

940 Hallegatte, S., Green, C., Nicholls, R.J. and Corfee-Morlot, J., 2013. Future flood losses in major coastal  
941 cities. *Nature climate change*, 3(9): 802-806.

942 Hirabayashi, Y. et al., 2013. Global flood risk under climate change. *Nature Climate Change*, 3(9): 816-821.

943 Hisdal, H. and Tallaksen, L.M., 2003. Estimation of regional meteorological and hydrological drought  
944 characteristics: a case study for Denmark. *Journal of Hydrology*, 281(3): 230-247.

945 Hutchinson, M.F. and Xu, T., 2004. Anusplin version 4.2 user guide. Centre for Resource and Environmental  
946 Studies. The Australian National University. Canberra, 5.

947 Javaheri, A. and Babbar-Sebens, M., 2014. On comparison of peak flow reductions, flood inundation maps,  
948 and velocity maps in evaluating effects of restored wetlands on channel flooding. *Ecological Engineering*,  
949 73: 132-145.

950 Jongman, B., 2018. Effective adaptation to rising flood risk. *Nature Communications*, 9(1): 1986.

951 Kharrufa, N.S., 1985. Simplified equation for evapotranspiration in arid regions. *Hydrologie Sonderheft*, 5(1):  
952 39 – 47.

953 Kriegler, E. et al., 2017. Fossil-fueled development (SSP5): An energy and resource intensive scenario for  
954 the 21st century. *Global Environmental Change*, 42: 297-315.

955 Kumar, P. et al., 2021. Nature-based solutions efficiency evaluation against natural hazards: Modelling  
956 methods, advantages and limitations. *Sci Total Environ*, 784: 147058.

957 Lee, S. et al., 2018. Assessing the cumulative impacts of geographically isolated wetlands on watershed  
958 hydrology using the SWAT model coupled with improved wetland modules. *Journal of Environmental*  
959 *Management*, 223: 37-48.

960 Liu, D., 2020. A rational performance criterion for hydrological model. *Journal of Hydrology*, 590: 125488.  
961 <https://doi.org/10.1016/j.jhydrol.2020.125488>.

962 Li, F., Zhang, G. and Xu, Y.J., 2014. Spatiotemporal variability of climate and streamflow in the Songhua  
963 River Basin, northeast China. *Journal of Hydrology*, 514: 53-64.

964 Li, W. et al., 2021. Where and how to restore wetland by utilizing storm water at the regional scale: A case  
965 study of Fangshan, China. *Ecological Indicators*, 122: 107246.

966 Lobligeois, F., Andréassian, V., Perrin, C., Tabary, P. and Loumagne, C., 2014. When does higher spatial  
967 resolution rainfall information improve streamflow simulation? An evaluation using 3620 flood events.  
968 *Hydrology and Earth System Sciences*, 18(2): 575-594.

969 Maes, J. et al., 2015. More green infrastructure is required to maintain ecosystem services under current  
970 trends in land-use change in Europe. *Landscape Ecology*, 30(3): 517-534.

971 Manfreda, S., Miglino, D. and Albertini, C., 2021. Impact of detention dams on the probability distribution  
972 of floods. *Hydrology and Earth System Sciences*, 25(7): 4231-4242.

973 Maraun, D., 2016. Bias Correcting Climate Change Simulations - a Critical Review. *Current Climate Change*  
974 *Reports*, 2(4): 211-220.

975 Martinez-Martinez, E., Nejadhashemi, A.P., Woznicki, S.A. and Love, B.J., 2014. Modeling the hydrological  
976 significance of wetland restoration scenarios. *Journal of Environmental Management*, 133: 121-134.

977 Melsen, L.A. et al., 2019. Subjective modeling decisions can significantly impact the simulation of flood and  
978 drought events. *Journal of Hydrology*, 568: 1093-1104.

979 Meng, B., Liu, J., Bao, K. and Sun, B., 2019. Water fluxes of Nenjiang River Basin with ecological network  
980 analysis: Conflict and coordination between agricultural development and wetland restoration. *Journal of*

981 Cleaner Production, 213: 933-943.

982 Moore, K., Pierson, D., Pettersson, K., Schneiderman, E. and Samuelsson, P., 2008. Effects of warmer world  
983 scenarios on hydrologic inputs to Lake Mälaren, Sweden and implications for nutrient loads. *Hydrobiologia*,  
984 599(1): 191-199.

985 Moriasi, D.N., 2007. Model Evaluation Guidelines for Systematic Quantification of Accuracy in Watershed  
986 Simulations. *Transactions of the ASABE*, 50(3): 885-900.

987 Moriasi, D.N., Gitau, M.W., Pai, N. and Daggupati, P., 2015. Hydrologic and water quality models:  
988 Performance measures and evaluation criteria. *Transactions of the ASABE*, 58(6): 1763-1785.

989 Moriasi, D.N., Gitau, M.W., Pai, N. and Daggupati, P., 2015. Hydrologic and water quality models:  
990 Performance measures and evaluation criteria. *Transactions of the ASABE*, 58(6): 1763-1785.

991 Muller, M., 2019. Hydropower dams can help mitigate the global warming impact of wetlands. *Nature*,  
992 566(7744): 315-317.

993 N. Moriasi, D. et al., 2007. Model Evaluation Guidelines for Systematic Quantification of Accuracy in  
994 Watershed Simulations. *Transactions of the ASABE*, 50(3): 885-900.

995 Nash, J.E. and Sutcliffe, J.V., 1970. River flow forecasting through conceptual models part I—A discussion  
996 of principles. *Journal of hydrology*, 10(3): 282-290.

997 Nelson, D.R., Bledsoe, B.P., Ferreira, S. and Nibbelink, N.P., 2020. Challenges to realizing the potential of  
998 nature-based solutions. *Current Opinion in Environmental Sustainability*, 45: 49-55.

999 Nika, C.E. et al., 2020. Nature-based solutions as enablers of circularity in water systems: A review on  
1000 assessment methodologies, tools and indicators. *Water Research*, 183: 115988.

1001 Noël, P., Rousseau, A.N., Paniconi, C. and Nadeau, D.F., 2014. Algorithm for delineating and extracting  
1002 hillslopes and hillslope width functions from gridded elevation data. *Journal of Hydrologic Engineering*,  
1003 19(2): 366-374.

1004 O'Neill, B.C. et al., 2016. The Scenario Model Intercomparison Project (ScenarioMIP) for CMIP6.  
1005 *Geoscientific Model Development*, 9(9): 3461-3482.

1006 Park, J., Botter, G., Jawitz, J.W. and Rao, P.S.C., 2014. Stochastic modeling of hydrologic variability of  
1007 geographically isolated wetlands: Effects of hydro-climatic forcing and wetland bathymetry. *Advances in*  
1008 *Water Resources*, 69: 38-48.

1009 Pool, S., Vis, M., Seibert, J. and Sveriges, L., 2018. Evaluating model performance: towards a non-parametric  
1010 variant of the Kling-Gupta efficiency. *Hydrological sciences journal*, 63(13-14): 1941-1953.

1011 Rajib, A., Golden, H.E., Lane, C.R. and Wu, Q., 2020. Surface Depression and Wetland Water Storage  
1012 Improves Major River Basin Hydrologic Predictions. *Water Resources Research*, 56(7): e2019WR026561.

1013 Rousseau, A.N. et al., 2011. PHYSITEL, a specialized GIS for supporting the implementation of distributed  
1014 hydrological models. *Water News-Official Magazine of the Canadian Water Resources Association*, 31(1):  
1015 18-20.

1016 Saharia, M. et al., 2017. Mapping Flash Flood Severity in the United States. *Journal of Hydrometeorology*,  
1017 18(2): 397-411.

1018 Schneider, C., Flörke, M., De Stefano, L. and Petersen-Perlman, J.D., 2017. Hydrological threats to riparian  
1019 wetlands of international importance - a global quantitative and qualitative analysis. *Hydrology and Earth  
1020 System Sciences*, 21(6): 2799-2815.

1021 Seibert, J., Vis, M.J.P., Lewis, E. and Meerveld, H.J., 2018. Upper and lower benchmarks in hydrological  
1022 modelling. *Hydrological Processes*, 32: 1120 - 1125.

1023 Shafeeque, M. and Luo, Y., 2021. A multi-perspective approach for selecting CMIP6 scenarios to project  
1024 climate change impacts on glacio-hydrology with a case study in Upper Indus river basin. *Journal of  
1025 Hydrology*, 599: 126466.

1026 Shook, K., Papalexiou, S. and Pomeroy, J.W., 2021. Quantifying the effects of Prairie depressional storage  
1027 complexes on drainage basin connectivity. *Journal of Hydrology*, 593: 125846.

1028 Smakhtin, V.U., 2001. Low flow hydrology: a review. *Journal of Hydrology*, 240(3): 147-186.

1029 Staudinger, M., Stahl, K., Seibert, J., Clark, M.P. and Tallaksen, L.M., 2011. Comparison of hydrological  
1030 model structures based on recession and low flow simulations. *Hydrology and Earth System Sciences*, 15(11):  
1031 3447-3459.

1032 Tallaksen, L.M. and van Lanen, H.A.J., 2004. Hydrological drought; processes and estimation methods for  
1033 streamflow and groundwater. *Developments in water science*, 48.

1034 Thorslund, J. et al., 2017. Wetlands as large-scale nature-based solutions: Status and challenges for research,  
1035 engineering and management. *Ecological Engineering*, 108: 489-497.

1036 Tolson, B.A. and Shoemaker, C.A., 2007. Dynamically dimensioned search algorithm for computationally

1037 efficient watershed model calibration. *Water Resources Research*, 43(1): 1-6.

1038 Turcotte, R., Fortin, L.G., Fortin, V., Fortin, J.P. and Villeneuve, J.P., 2007. Operational analysis of the  
1039 spatial distribution and the temporal evolution of the snowpack water equivalent in southern Québec, Canada.  
1040 *Hydrology Research*, 38(3): 211-234.

1041 UNISDR, C., 2015. The human cost of natural disasters: A global perspective.

1042 van Vuuren, D.P. et al., 2017. The Shared Socio-economic Pathways: Trajectories for human development  
1043 and global environmental change. *Global Environmental Change*, 42: 148-152.

1044 Walz, Y. et al., 2021. Disaster-related losses of ecosystems and their services. Why and how do losses matter  
1045 for disaster risk reduction? *International Journal of Disaster Risk Reduction*, 63: 102425.

1046 Wang, L., Chen, X., Shao, Q. and Li, Y., 2015. Flood indicators and their clustering features in Wujiang  
1047 River, South China. *Ecological Engineering*, 76: 66-74.

1048 Wang, S., Zhang, L., She, D., Wang, G. and Zhang, Q., 2021. Future projections of flooding characteristics  
1049 in the Lancang-Mekong River Basin under climate change. *Journal of Hydrology*, 602: 126778.

1050 Wang, X., Yang, W. and Melesse, A.M., 2008. Using Hydrologic Equivalent Wetland Concept Within  
1051 SWAT to Estimate Streamflow in Watersheds with Numerous Wetlands. *Transactions of the ASABE*, 51(1):  
1052 55-72.

1053 Ward, P.J. et al., 2020. The need to integrate flood and drought disaster risk reduction strategies. *Water  
1054 Security*, 11: 100070.

1055 Wu, Y., Zhang, G., Rousseau, A.N. and Xu, Y.J., 2020. Quantifying streamflow regulation services of  
1056 wetlands with an emphasis on quickflow and baseflow responses in the Upper Nenjiang River Basin,  
1057 Northeast China. *Journal of Hydrology*, 583: 124565.

1058 Wu, Y., Zhang, G., Rousseau, A.N., Xu, Y.J. and Foulon, É., 2020. On how wetlands can provide flood  
1059 resilience in a large river basin: A case study in Nenjiang river Basin, China. *Journal of Hydrology*, 587:  
1060 125012.

1061 Wu, Y., Zhang, G., Xu, Y.J. and Rousseau, A.N., 2021. River Damming Reduces Wetland Function in  
1062 Regulating Flow. *Journal of Water Resources Planning and Management*, 147(10).

1063 Xu, X. et al., 2019. Evaluating the impact of climate change on fluvial flood risk in a mixed-use watershed.  
1064 *Environmental Modelling & Software*, 122: 104031.

1065 Yassin, F. et al., 2019. Representation and improved parameterization of reservoir operation in hydrological  
1066 and land-surface models. *Hydrology and Earth System Sciences*, 23(9): 3735-3764.

1067 Zedler, J.B. and Kercher, S., 2005. WETLAND RESOURCES: Status, Trends, Ecosystem Services, and  
1068 Restorability. *Annual Review of Environment and Resources*, 30(1): 39-74.

1069 Zelenhasić, E. and Salvai, A., 1987. A method of streamflow drought analysis. *Water resources research*,  
1070 23(1): 156-168.

1071 Zeng, L., Shao, J. and Chu, X., 2020. Improved hydrologic modeling for depression-dominated areas. *Journal*  
1072 *of Hydrology*, 590: 125269.

1073 Zhang, X. and Song, Y., 2014. Optimization of wetland restoration siting and zoning in flood retention areas  
1074 of river basins in China: A case study in Mengwa, Huaihe River Basin. *Journal of Hydrology*, 519: 80-93.

1075 Zhao, G., Gao, H., Naz, B.S., Kao, S. and Voisin, N., 2016. Integrating a reservoir regulation scheme into a  
1076 spatially distributed hydrological model. *Advances in Water Resources*, 98: 16-31.

1077 Zhao, Y. et al., 2021. Future precipitation, hydrology and hydropower generation in the Yalong River Basin:  
1078 Projections and analysis. *Journal of Hydrology*, 602: 126738.

1079